Journal of Statistical Physics, Vol. 67, Nos. 5/6, 1992

Optimized Analysis of the Critical Behavior in Polymer Mixtures from Monte Carlo Simulations

Hans-Peter Deutsch[1]

Received October 4, 1991; final February 21, 1992

A complete outline is given for how to determine the critical properties of polymer mixtures with extrapolation methods similar to the Ferrenberg–Swendsen techniques recently devised for spin systems. By measuring not only averages but the whole distribution of the quantities of interest, it is possible to extrapolate the data obtained in only a few simulations near T_c over the entire critical region, thereby saving at least 90% of the computer time normally needed to locate susceptibility peaks or cumulant intersections and still getting more precise results. A complete picture of the critical properties of polymer mixtures in the thermodynamic limit is then obtained with finite-size scaling functions. Since the amount of information extracted from a simulation in this way is drastically increased as compared to conventional methods, the investigation of mixtures with long chains or built-in asymmetries is now possible. As an example, the critical points, exponents, and amplitudes of dense, symmetric polymer mixtures with chain lengths ranging from $N=16$ up to $N=256$ are determined within the framework of the 3D bond fluctuation model using grand canonical simulation techniques. As an example for an asymmetry, the generalization of the method to asymmetric monomer potentials is briefly discussed.

KEY WORDS: Polymer mixture; histogram method; finite-size scaling; phase transition; Monte Carlo.

1. INTRODUCTION

Polymer melts and blends have been the subject of intensive scientific investigation over many years. Although polymers of different chemical nature are generally very incompatible due to the very little entropy gain of such mixtures[1] as opposed to the entropy gain in mixtures of small molecules, there is a large practical interest in mixing polymers with different properties to get new materials with sometimes exciting features,

[1] Institut für Physik, Johannes-Gutenberg-Universität, D-6500 Mainz, Germany.

0022-4715/92/0600-1039$06.50/0

and in material sciences and industry, polymer blends are a field of major interest. Various experimental methods are available and have been used extensively to measure the entropies and enthalpies of mixing,[2] the effective interaction parameters,[3,4] and the phase diagrams, i.e., the coexistence curves for phase separation and spinodal curves[5,7] in polymer blends. When compared with the existing analytic theories such as the Flory–Huggins lattice model[1,8,9] or generalizations thereof,[10–12] which are all mean-field theories, the experimental findings often are in blatant contrast to major predictions of those theories. One prominent example of these discrepancies is the Flory–Huggins interaction parameter χ. This parameter has been determined experimentally for many systems by fitting the theoretical Flory–Huggins expression for the free energy of mixing per particle[1]

$$\frac{\Delta F}{k_B T} = \frac{\phi_A}{N_A} \ln(\phi_A) + \frac{\phi_B}{N_B} \ln(\phi_B) + \phi_v \ln(\phi_v) + \chi \phi_A \phi_B \tag{1}$$

to the experimental data on phase separation, heat of mixing, or extrapolated zero-angle neutron scattering, using χ as a free parameter. While according to the mean-field theories χ in Eq. (1) should be a purely enthalpic quantity $\sim T^{-1}$, independent of composition (polymer densities), experiments generally find that their effective Flory parameters contain strong composition dependences.[3,4] Another point which has been in particular focus recently is that the analytic theories naturally predict mean-field critical behavior for the (second-order) unmixing transition, while according to the Ginzburg criterion[13–16] there should be non-mean-field (Ising) behavior very near the critical point. This non-mean-field critical behavior has been demonstrated nicely by recent small-angle neutron and dynamic light scattering experiments[17] and has also been seen in various Monte Carlo simulations.[18,19] Even though Monte Carlo methods[20–23]—like the analytic theories—use lattice models, their results are in far better qualitative agreement with the experimental findings. They show, for instance, strong composition dependences of the effective Flory parameter and non-mean-field critical behavior at the unmixing transition. Therefore the use of a lattice in describing polymer systems is presumably not a severe error and the failure of the analytic theories stems from various other crude approximation.[18]

In the light of these aspects one might ask why there are so very few Monte Carlo approaches to polymer mixtures. The reason is that there are three very severe hindrances which have made Monte Carlo simulation of polymer blends practically impossible until very recently.

(a) To see the unmixing transition occur just by the diffusive motion of the polymers[24–27] is impossible within any reasonable amount

of computer time. Even if this time were available, the lattices which can be simulated are for long chains by far too small to allow the system to form domains of different phases.

(b) Since relaxation times near the critical point are very large and acceptance rates in dense systems are usually small, one has to wait extremely long (in units of CPU time) between two uncorrelated measurements of, for instance, the order parameter of the transition.

(c) The physically interesting case of mixing polymer species with different properties, such as different stiffnesses or bond lengths, is almost impossible to model using convential lattice algorithms,[20,21,28,29] which usually provide only one bond length (the lattice spacing) and two bond angles (π and $\pi/2$).

While previous simulations of polymer mixtures[18,19] could overcome the first difficulty by simulating in a grand canonical rather than a canonical ensemble, they could not get around the second and third points and therefore restricted their investigations to rather dilute systems with short chains where the two polymer species A and B were exactly equal. Upper critical solution temperatures in these so-called *symmetric* polymer mixtures due to a small repulsive potential between species A and B and parabolicly shaped density dependences of the effective χ parameter have been found in these simulations as well as in recent experiments.[30] But many important questions had to remain unanswered due to the second and third difficulties, for instance, whether the observed completely Ising-like critical behavior over the whole scaling region is an artefact of the short chains or how the critical points get shifted in asymmetric mixtures.

While by now, with the advent of new sophistaced lattice algorithms such as the bond fluctuation model in two[31] and three[26,25,32] dimensions, point (c) is in principle no longer a real problem, there remains the fundamental difficulty (b).

In this paper I present methods to overcome this difficulty. Since the problem of long relaxation times for long chains, especially near a critical point, is of fundamental and general (model-independent) nature, (marginal) improvement of the algorithms seems not to be the most promising strategy. A different, complementary approach is to increase the amount of information extracted from a simulation run. Conventionally averages of certain quantities relevant for the phase transition, such as order parameter, susceptibility, specific heat, etc., are measured. But this is by far not all the information generated by the simulation! Much more information can be achieved by storing the complete distributions instead of just the averages (first few moments) of the quantities in question. The

drastically larger amount of information contained in these distributions (*histograms*) can then be used to calculate the behavior of the system over a whole range of the relevant parameters (temperature and chemical potential, say). The idea of storing whole distributions has a long history[33,34] and has recently been revived by Ferrenberg and Swendsen[35] for spin systems. Here I introduce this method for polymers and in addition present some new methods to analyze the data in the framework of finite-size scaling to obtain the complete critical behavior of polymer mixtures including critical exponents and amplitudes. The systems used to demonstrate the above ideas are symmetric polymer mixtures in three dimensions simulated with the already mentioned bond fluctuation model.[26] Asymmetry can easily be implemented in the model by introducing different potentials for the bond angles, bond lengths, or monomer–monomer interactions of the two species and is indeed under current investigation.[36] The methods apply with only slight generalizations, which are described briefly in Section 3, directly to the asymmetric case, too.

The remainder of this paper is organized as follows. In Section 2, I present the grand canonical method, necessary to overcome difficulty (a), for our model and derive the partition function for the simulated ensemble. In Section 3 the histogram extrapolation techniques for polymers are introduced and compared with conventional Monte Carlo data. In Section 4, I present useful functions following from finite-size scaling considerations by which one can determine all critical properties of the mixtures with reasonable accuracy even for long chains. Section 5 contains some concluding remarks and an outlook for future studies.

2. GRAND CANONICAL SIMULATIONS

The simulated systems live on 3D simple cubic lattices with size L^3 ranging from $L=24$ up to 112 to take finite-size effects into account properly. These lattices are filled with chains of two species called A and B at a volume fraction $\phi=0.5$ corresponding to real systems with density ~ 0.8,[25] i.e., dense melts. The simulated chain lengths N_A and N_B of the A and B chains range from 16 to 256. For the symmetric case considered here one always has $N_A=N_B\equiv N$. In the three-dimensional bond fluctuation model[26,32] each effective monomer occupies one unit cell of the lattice (eight lattice sites) and the bonds between the monomers of one polymer may have all possible lengths from 2 to $\sqrt{10}$ omitting the length $\sqrt{8}$. With this set of allowed bonds the self-avoiding condition (no two monomer corners may sit on the same site) automatically ensures that bonds cannot intersect in the course of their motion, and thus entanglement constraints

are fully incorporated.[26,36] The *canonical* motion of the polymers consists of random diffusive jumps of their monomers to a nearest-neighbor lattice site, subject to excluded volume and the bond constraints. The effect of interaction potentials is taken into account by the usual Metropolis transition rate $\min\{1, \exp(-\Delta E/k_B T)\}$, where ΔE is the energy change induced by the move. It can be shown[26] that within this model five different bond lengths and 87 different bond angles occur in the simulation, so there are indeed many possibilities for modeling varying polymer properties via suitable potential energies.

The monomer interaction potentials used in this study are square-well potentials ranging over the entire first peak of the pair correlation,[26] i.e., over the first three neighbor shells (54 lattice sites) up to a distance $\sqrt{6}$. The effective coordination number q of this particular system is $q = 14$.[26] The strengths of the potential are

$$\varepsilon_{AA} = \varepsilon_{BB} = -\varepsilon_{AB} \equiv -\varepsilon \tag{2}$$

resulting in spontaneous decomposition of the mixture below a critical temperature T_c. An appropriate and natural order parameter to quantify this phase transition is the difference between the numbers n_A of A chains and n_B of B chains,

$$m = M/n, \qquad \text{with} \quad M \equiv n_A - n_B, \quad n \equiv n_A + n_B \tag{3}$$

With ϕ_c denoting the critical density at the unmixing transition, the order parameter is related to the monomer densities ϕ_A, ϕ_B of the symmetrical mixtures via

$$\phi_A = \phi_c(1+m), \qquad \phi_B = \phi_c(1-m), \qquad \phi_c = (1-\phi_v)/2 \tag{4}$$

To accelerate the unmixing process a *grand canonical* MC step, where each polymer may switch its identity $A \leftrightarrow B$, is performed after each canonical MC step (attempted diffusive jump of each monomer). The question of the relative weights of those two processes, i.e., after how many canonical moves a grand canonical move may be attempted, in general is a delicate matter because the chains must have enough time to relax after the switches. This time may be very large for strong asymmetries or far below the unmixing transition point, but in the present case, where A and B chains are completely equal and we are interested in the critical region near the transition where also the densities ϕ_A and ϕ_B are approximately the same, differences between the chaim configurations of A and B are negligible to a very high degree of accuracy and a relabeling step can be performed after each canonical MC step.[18] Clearly, in such an ensemble

the order parameter M *is not* conserved, whereas the total number n of chains *is* conserved. Such a system is neither canonical (both n and M conserved) nor strictly grand canonical (both n and M *not* conserved) and strictly speaking one should put the words "grand canonical" in the title of this section in quotation marks. A detailed understanding of the partition function of such an ensemble is necessary for (a) defining an appropriate transition probability for the relabeling step and (b) applying the histogram analysis described in the next section.

Let c denote one configuration of the system (position and identity of every monomer fixed). The microcanonical (n and M and internal energy E conserved[37]) partition function

$$\Gamma(E, M) = \sum_c \delta(E(c) - E)\, \delta(M(c) - M) \tag{5}$$

is the number of configurations with energy E and order parameter M and will therefore also be called the phase space volume or density of states. To get from the microcanonical to the canonical ensemble one has to integrate with the Boltzmann measure $e^{-\beta E}\, dE$ with $\beta = 1/k_B T$. This yields the free energy F of the system:

$$e^{-\beta F} \equiv \int dE\, e^{-\beta E} \Gamma(E, M) \tag{6}$$

This canonical partition function integrated with the measure $\exp[\beta N(\mu_A n_A + \mu_B n_B)]\, dn_A\, dn_B$ yields the partition function of the true grand canonical ensemble where the chemical potentials per monomer μ_A, μ_B are conserved but neither n_A nor n_B is. This is a more general ensemble than the simulated systems are, where the total number of chains is held fixed. This constraint can be taken into account by including a factor $\delta(n_A + n_B - n)$ in the grand canonical measure, leading to

$$\mathcal{Z}(N, \beta, \mu_A, \mu_B) = \int_{-n}^{n} dM \int dE\, e^{\beta N[n(\mu_A + \mu_B) + M(\mu_A - \mu_B)]/2} e^{-\beta E} \Gamma(E, M)$$

Now observe that the factor $\exp\{\beta N[n(\mu_A + \mu_B)]/2\}$ is independent of the integration variables and can be written in front of all integrations. Such a factor in the partition function is irrelevant, since it cancels in any expression for physical quantities (averages). Therefore the constraint of fixed n also implies that there are no two independent chemical potentials μ_A, μ_B, but only their difference

$$\Delta\mu \equiv \mu_A - \mu_B \tag{7}$$

matters. The final form of the partition function appropriate for the simulated systems then reads

$$\mathcal{Z}(N, \beta, \Delta\mu) = \int_{-n}^{n} dM \int dE\, e^{\beta\Delta\mu MN/2} e^{-\beta E} \Gamma(E, M) \tag{8}$$

An analytic expression like (8) for the partition function of the systems in question is always an indispensable necessity if one wants to apply histogram methods for the data analysis. It is also easy to derive a proper transition probability for the Monte Carlo steps once $\mathcal{Z}$ is available: A transition probability $W(c \to c')$ to go from a configuration c to another one c' has to obey detailed balance[38,39] which is trivially fulfilled, for instance, for the Metropolis transition $W(c \to c') = \min\{1, P(c')/P(c)\}$.[38] The probability $P(c)$ of a configuration c can be read off directly from the partition function

$$P(c) = \mathcal{Z}(N, \beta, \Delta\mu)^{-1} e^{\beta\Delta\mu M(c)N/2} e^{-\beta E(c)}$$

and the Metropolis transition probability for any Monte Carlo move can be written down. For instance, for the "grand canonical" relabeling of a chain

$$W(c \to c') = \min\{1, e^{-\beta(\Delta E \pm N\Delta\mu)}\} \tag{9}$$

where ΔE is the energy change induced by the switch and the plus sign in front of $\Delta\mu$ applies to a switch $A \to B$, whereas the minus sign applies to $B \to A$. The parameters β and $\Delta\mu$ can be chosen as desired. When compared to a corresponding magnetic system where an A-polymer corresponds to an up spin and a B-polymer to a down spin, the quantity $N\Delta\mu$ corresponds to the external magnetic field.

3. HISTOGRAMS AND EXTRAPOLATIONS

3.1. Single-Hisogram Analysis

As emphasized in the Introduction, the key idea of the Ferrenberg–Swendsen method is to obtain as much information as possible about the critical phenomena of the mixtures not only by measuring the first few moments of the order prameter and the internal energy, but by recording the whole histogram $H(E, M)$, i.e., storing the number of occurrences of any pair (E, M) measured during the simulations. Figure 1 shows such a histogram for a mixture of chains with length $N = 32$ near the critical point. Those histograms approach the probability distribution $P(E, M)$ in the

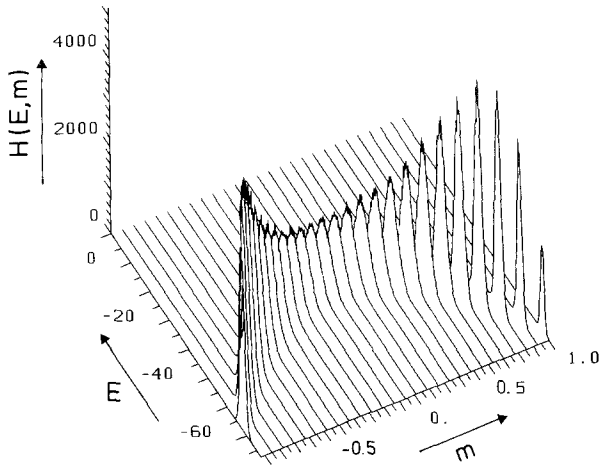

Fig. 1. Measured histogram of a mixture with chain length $N=32$ and system size $L=24$ from a simulation at $(T, \Delta\mu)=(69.3, 0)$. Each line represents the (unnormalized) energy distribution for a fixed order parameter.

limit $\mathcal{N} \to \infty$, where $\mathcal{N}$ denotes the number of independent measurements. Because an analytic expression for the partition function is known [see Eq. (8)], the distribution $P(E, M)$ can be related to the phase space volume (5):

$$\mathcal{N}^{-1} H_{\beta,\mu}(E, M) \approx P_{\beta,\mu}(E, M) = \mathcal{Z}(n, \beta, \mu)^{-1} e^{\beta\Delta\mu MN/2} e^{-\beta E} \Gamma(E, M) \qquad (10)$$

This equation can be solved to yield an approximation for Γ out of the simulation at one particular point $(\beta, \Delta\mu)$ in parameter space. Now the crucial point is that the density of states $\Gamma(E, M)$ is *independent* of the parameters β and $\Delta\mu$ (inverse temperature and chemical potential). So the approximation for the phase space volume can be inserted into any expression containing Γ, even if this expression is evaluated at parameters $(\beta', \Delta\mu')$ different from the simulation point. For instance, when inserted into Eq. (8) one gets an approximation for the partition function at $(\beta', \Delta\mu')$:

$$\mathcal{Z}(N, \beta', \Delta\mu') \approx \mathcal{N}^{-1} \mathcal{Z}(N, \beta, \Delta\mu) \int dM \int dE\, e^{(\beta'\Delta\mu' - \beta\Delta\mu)MN/2} e^{-(\beta'-\beta)E} H_{\beta,\Delta\mu}(E, M) \qquad (11)$$

Note that this expression still contains $\mathcal{Z}(N, \beta, \Delta\mu)$, the unknown partition

function at the simulation point. But this is just a constant factor with respect to the parameters $(\beta', \Delta\mu')$ and reflects the impossibility of determining the zero of the entropy. In fact this unknown factor even cancels out in the approximation for the probability distribution of E and M:

$$\begin{aligned} P_{\beta',\Delta\mu'}(E, M) &\equiv \mathcal{Z}(N, \beta', \Delta\mu')^{-1} e^{\beta'\Delta\mu' MN/2} e^{-\beta' E} \Gamma(E, M) \\ &\approx \frac{\mathcal{Z}(N, \beta, \Delta\mu)}{\mathcal{N}\mathcal{Z}(N, \beta', \Delta\mu')} e^{(\beta'\Delta\mu' - \beta\Delta\mu)MN/2} e^{-(\beta' - \beta)E} H_{\beta,\Delta\mu}(E, M) \\ &\approx \frac{H_{\beta,\Delta\mu}(E, M) e^{(\beta'\Delta\mu' - \beta\Delta\mu)MN/2} e^{-(\beta' - \beta)E}}{\int dM \int dE\, H_{\beta,\Delta\mu}(E, M) e^{(\beta'\Delta\mu' - \beta\Delta\mu)MN/2} e^{-(\beta' - \beta)E}} \end{aligned} \tag{12}$$

Using both approximations (10) and (11) for Γ and $\mathcal{Z}$ nicely cancels all unknown partition functions. Having an approximation for the distribution, one can immediately write down the corresponding equation for the average of any function $f(E, M)$:

$$\begin{aligned} &\langle f(E, M) \rangle_{\beta',\Delta\mu'} \\ &\quad \equiv \int dM \int dE\, f(E, M)\, P_{\beta',\Delta\mu'}(E, M) \\ &\quad \approx \frac{\int dM \int dE\, f(E, M)\, H_{\beta,\Delta\mu}(E, M)\, e^{(\beta'\Delta\mu' - \beta\Delta\mu)MN/2} e^{-(\beta' - \beta)E}}{\int dM \int dE\, H_{\beta,\Delta\mu}(E, M)\, e^{(\beta'\Delta\mu' - \beta\Delta\mu)MN/2} e^{-(\beta' - \beta)E}} \end{aligned} \tag{13}$$

Thus, extrapolations to any parameter combination in the vicinity of the simulated parameter point for any function of the quantities (here E and M) for which the histogram was recorded are possible. Of course, one should not extrapolate too far away from the simulation point because then the Boltzmann weights in Eqs. (11)–(13) emphasize values of (E, M) far out in the wings of the measured histogram where the statistics is poor. The best region to use histogram methods is in fact the critical region since there the specific heat and the order parameter susceptibility get very large and the histogram [distribution of (E, M)] becomes very broad and therefore suitable for extrapolations. It can be argued[35] that the region of validity of the single-histogram method just coincides with the scaling region.

Recently it has been suggested to not use the whole histogram for extrapolations but a series expansion involving only the first few cumulants.[40] By this one can avoid mainly using the wings of the measured histogram far away from the simulation point and therefore extrapolations obtained with this cumulant method may be valid over

a wider parameter range. The questions of errors and valid ranges of all these extrapolation schemes are delicate matters and still under active investigation.

3.2. Entropy and Free Energy

As already mentioned, the histogram analysis via Eq. (11) automatically yields (up to a constant factor) an estimate for the partition function of the system, a quantity usually not accessible in simulations. Therefore all thermodynamic quantities such as the entropy or the free energy which follow directly from the logarithm of $\mathscr{Z}$ can be determined up to an additive constant.

To see how this works in general, let $Z \equiv \sum e^{-\beta\psi}$ be the partition function of some arbitrary statistical ensemble and let $P \equiv Z^{-1} e^{-\beta\psi}$ be the probability of one state of that ensemble. For instance, in a canonical ensemble we would have $\sum = \sum_c$ and $\psi = \mathscr{H}(c)$, in the ensemble of Eq. (8) we have $\sum = \int dM \int dE\, \Gamma(E, M)$ and $\psi = E - \Delta\mu MN/2$. The entropy can be defined as

$$\begin{aligned} S &\equiv -k_B \sum P \ln P \\ &= k_B \beta \langle \psi \rangle + k_B \ln Z = -k_B \beta^2 \frac{\partial}{\partial \beta} (\beta^{-1} \ln Z) \end{aligned} \tag{14}$$

For the ensemble of Eq. (8) simulated here the histogram extrapolations (11) and (13) yield as an estimate for the entropy

$$\begin{aligned} &S(N, \beta', \Delta\mu') \\ &= k_B \beta' \langle E \rangle_{\beta'\Delta\mu'} - \frac{N}{2} k_B \beta' \Delta\mu' \langle M \rangle_{\beta'\Delta\mu'} + k_B \ln \mathscr{Z}(N, \beta', \Delta\mu') \\ &\approx k_B \beta' \frac{\int dM \int dE\, (E - \Delta\mu' MN/2)\, H_{\beta,\Delta\mu}(E, M)\, e^{(\beta'\Delta\mu' - \beta\Delta\mu)MN/2} e^{-(\beta' - \beta)E}}{\int dM \int dE\, H_{\beta,\Delta\mu}(E, M)\, e^{(\beta'\Delta\mu' - \beta\Delta\mu)MN/2} e^{-(\beta' - \beta)E}} \\ &\quad + k_B \ln \left[\int dM \int dE\, H_{\beta,\Delta\mu}(E, M)\, e^{(\beta'\Delta\mu' - \beta\Delta\mu)MN/2} e^{-(\beta' - \beta)E} \right] \\ &\quad + k_B \ln \left(\frac{\mathscr{Z}(N, \beta, \Delta\mu)}{\mathscr{N}} \right) \end{aligned} \tag{15}$$

Now the last term is the undetermined additive constant. A natural way to

define this constant (the zero of the entropy) is to fix the scale of the partition function such that

$$\mathscr{Z}(N, \beta, \Delta\mu) \equiv \mathscr{N} \tag{16}$$

i.e., such that the partition function at the simulation point is just the number of measurements taken at that point.[36] The motivation for this can be seen by comparing Eq. (13) with Eq. (11). The denominator in the estimated average of Eq. (13) in this normalization is just the estimated partition function from Eq. (11) and the extrapolation equation has the usual form of an ensemble average. The relation between the estimated partition functions in this normalization (denoted by $\bar{\mathscr{Z}}$) and the true partition function $\mathscr{Z}$ also follows from Eq. (11):

$$\bar{\mathscr{Z}}(N, \beta', \Delta\mu') \xrightarrow{\mathscr{N}\to\infty} \frac{\mathscr{N}\mathscr{Z}(N, \beta', \Delta\mu')}{\mathscr{Z}(N, \beta, \Delta\mu)} \tag{17}$$

With the scale of the partition function fixed, the estimates for the entropy S and the free energy F at parameters $(\beta', \Delta\mu')$ obtained from a simulation at $(\beta, \Delta\mu)$ read

$$k_B^{-1}\bar{S}(N, \beta', \Delta\mu') = +\ln \bar{\mathscr{Z}} - \beta'\Delta\mu'\langle M\rangle_{\beta'\Delta\mu'}N/2 + \beta'\langle E\rangle_{\beta'\Delta\mu'} \tag{18}$$

$$\beta\bar{F}(N, \beta', \Delta\mu') = -\ln \bar{\mathscr{Z}} + \beta'\Delta\mu'\langle M\rangle_{\beta'\Delta\mu'}N/2 \tag{19}$$

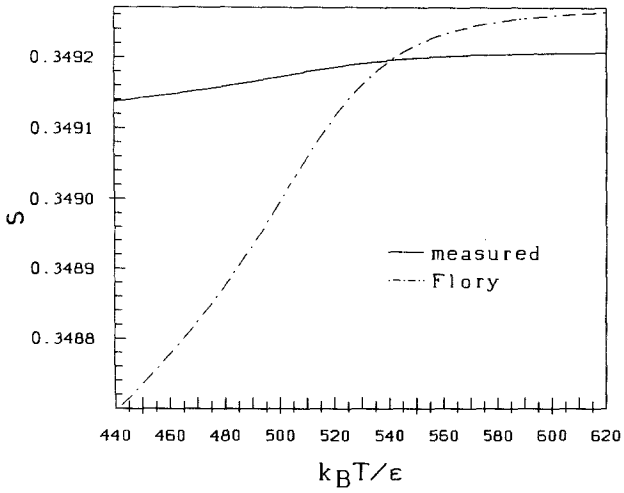

Fig. 2. Entropy of mixing (—) and Flory entropy of mixing (– · –) for mixtures with $N = 256$ and $L = 112$ as a function of temperature.

The free energy follows from $F = \langle E \rangle - TS$. A bar over a quantity means the quantity in the normalization (16). Observe that the free energy is *not* $-\beta^{-1} \ln \mathscr{Z}$, because the ensemble is not canonical. By definition F is always $\sim -\ln \sum e^{-\beta \mathscr{H}}$. The term $\sim \langle M \rangle$ in Eq. (19) just cancels the part of $\ln \mathscr{Z}$ which comes from the fugacity $e^{\beta \Delta \mu MN/2}$ in Eq. (8). This reflects the formal difference between this ensemble and the corresponding (canonical) magnetic system where the interaction with the external field belongs to the Hamiltonian so that there is no fugacity. Figures 2 and 3 show estimates from Eq. (18) for the entropy as a function of temperature and of the chemical potential difference in the critical region for symmetric polymer mixtures compared to the Flory ansatz (1). The densities ϕ_A, ϕ_B needed in Eq. (1) are obtained from extrapolations of the order parameter [see Eq. (4)]. Even though the finite-size effects in this region prevent a quantitative comparison, it seems that the Flory entropy does not even qualitatively describe the systems. To my knowledge this is the first *direct* test of Eq. (1), which is the starting point of the Flory–Huggins mean-field theories and many of its modifications.

3.3. Multiple-Histogram Analysis

Even though extrapolations from a single histogram obtained at one parameter combination $(\beta, \Delta\mu)$ already yield very good results if the histogram has good statistics and if the simulation point is near the critical

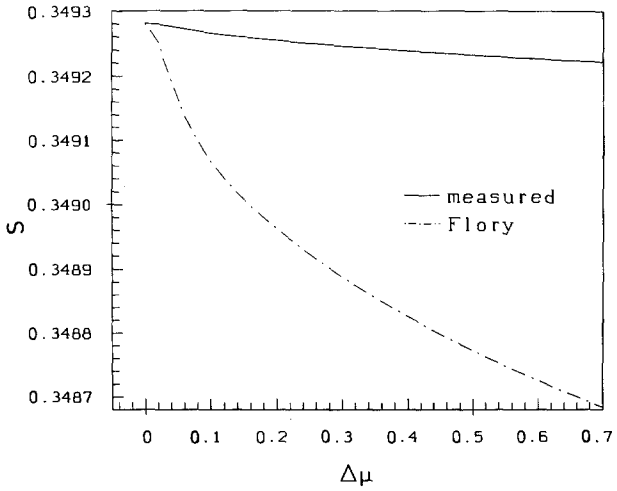

Fig. 3. Entropy of mixing (—) and Flory entropy of mixing (– · –) for mixtures with $N = 256$ and $L = 112$ as a function of chemical potential.

point so that the histogram is broad, it is often desirable to combine histograms from several simulations either to get extrapolations over a wider parameter range or just to increase the accuracy if several histograms are available.[35] If s simulations were performed at parameters $\{(\beta_i, \Delta\mu_i), i = 1,..., s\}$ the generalization for the basic equation (10), i.e., for the estimate of the parameter-independent phase space volume, reads

$$\Gamma(E, M) \approx \sum_{i=1}^{s} w_i(E, M)\, \mathcal{N}_i^{-1} \mathcal{Z}(N, \beta_i, \Delta\mu_i)\, e^{-\beta_i \Delta\mu_i MN/2} e^{\beta_i E} H_{\beta_i, \Delta\mu_i}(E, M) \tag{20}$$

where the weight w_i by which the histogram $H_{\beta_i, \Delta\mu_i}$ enters can be determined by the requirement that the statistical error $\Delta\Gamma$ of the estimate should be as small as possible. This error stems from the errors of the measured histograms

$$\Delta H_{\beta_i, \Delta\mu_i}(E, M) = [(1 + 2\tau_i)\, H_{\beta_i, \Delta\mu_i}(E, M)]^{1/2} \tag{21}$$

where τ_i is the autocorrelation time during the simulation i. This time can be determined in the usual way[41,42] by measuring the autocorrelations of M and E (see Fig. 4). τ can be set to zero here and in the folowing equations if one waits long enough between two measurements during the simulations. But in fact this is not even necessary since the τ_i cancel in the relevant equations (23) if they are equal. If not, they can also be ignored

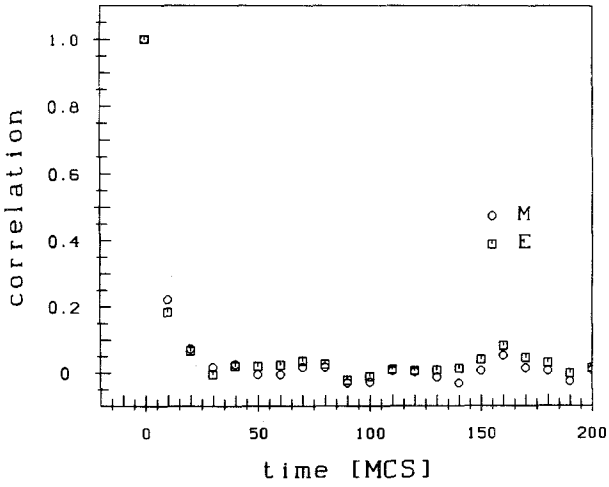

Fig. 4. Autocorrelations of order parameter (circles) and internal energy (squares) for a mixture with $N = 256$ and $L = 112$ at the critical point.

if they are only *roughly* equal, since the results, Eqs. (23), do not depend strongly on them.

The optimal weights w_i now follow from minimizing the error $\Delta\Gamma$ induced by the error ΔH by varying the w_i in Eq. (20). This variation can be done analytically[43] and yields the optimal weights

$$w_i(E, M) = \frac{(1+2\tau_i)^{-1} \mathcal{N}_i \mathcal{Z}(N, \beta_i, \Delta\mu_i)^{-1} e^{\beta_i(\Delta\mu_i MN/2 - E)}}{\sum_{j=1}^{s} (1+2\tau_j)^{-1} \mathcal{N}_j \mathcal{Z}(N, \beta_j, \Delta\mu_j)^{-1} e^{\beta_j(\Delta\mu_j MN/2 - E)}} \tag{22}$$

With this expression for the w_i everything except the partition functions at the simulation points is known in the estimate (20) for the phase space volume and one can proceed in a similar way as in the single-histogram case to get extrapolations for the partition function, the distribution, and averages at an arbitrary parameter combination $(\beta', \Delta\mu')$:

$$\begin{aligned}
\Gamma(E, M) &\approx X(E, M)/Y(E, M) \\
\mathcal{Z}(N, \beta', \Delta\mu') &\approx \int dM \int dE\, e^{\beta'(\Delta\mu' MN/2 - E)} X(E, M)/Y(E, M) \\
P_{\beta', \Delta\mu'}(E, M) &\approx \frac{e^{\beta'(\Delta\mu' MN/2 - E)} X(E, M)/Y(E, M)}{\int dM' \int dE'\, e^{\beta'(\Delta\mu' M'N'/2 - E')} X(E', M')/Y(E', M')} \\
\langle f(E, M)\rangle_{\beta', \Delta\mu'} &\approx \frac{\int dM \int dE\, f(E, M)\, e^{\beta'(\Delta\mu' MN/2 - E)} X(E, M)/Y(E, M)}{\int dM' \int dE'\, e^{\beta'(\Delta\mu' M'N'/2 - E')} X(E', M')/Y(E', M')}
\end{aligned} \tag{23}$$

To shorten the notation I introduced the abbreviations

$$\begin{aligned}
X(E, M) &:= \sum_{j=1}^{s} \frac{H_{\beta_j, \Delta\mu_j}(E, M)}{1+2\tau_j} \\
Y(E, M) &:= \sum_{j=1}^{s} \frac{\mathcal{N}_j e^{\beta_j(\Delta\mu_j MN/2 - E)}}{(1+2\tau_j)\, \mathcal{Z}(N, \beta_j, \Delta\mu_j)}
\end{aligned} \tag{24}$$

Now observe that the multiple-histogram equations (23) can be obtained directly from the single-histogram equations (11)–(13) by the simple and very natural substitution

$$\begin{aligned}
H_{\beta, \Delta\mu}(E, M) &\to X(E, M) \\
\frac{\mathcal{N} e^{\beta(\Delta\mu MN/2 - E)}}{\mathcal{Z}(N, \beta, \Delta\mu)} &\to Y(E, M)
\end{aligned} \tag{25}$$

To see this, however, one should not cancel factors $\sim \mathcal{N}\mathcal{Z}(N, \beta, \Delta\mu)$ in the derivation of the single-histogram equations to identify all the terms on

which the transformation (25) has to be applied.[36] This is one sign of the principally more information contained in the multiple-histogram approach. This fact clearly shows up also at the errors of the extrapolations. The relative statistical error of the extrapolated distribution is given by[35]

$$\frac{\Delta P_{\beta',\Delta\mu'}(E, M)}{P_{\beta',\Delta\mu'}(E, M)} = \left[\sum_{j=1}^{s} (1 + 2\tau_j)^{-1} H_{\beta_j,\Delta\mu_j}(E, M) \right]^{-1/2} \tag{26}$$

and can only get smaller with each additional histogram. As an example for an extrapolated distribution, Fig. 5 shows the order parameter distribution $P(M) = \int dE\, P(E, M)$ for a mixture of chains with length $N = 256$ on a lattice of size 112^3 in the critical region. For this extrapolation five histograms obtained at the parameter points $(T, \Delta\mu) = (525.0, 0)$, $(531, 0)$, $(531, 0.281)$, $(541, 0)$ with roughly 10^4 independent measurements at each point were used.

3.4. Self-Consistent Determination of the Partition Function

Since the partition functions at the simulation points now appear in sums over the simulation points [see Eq. (24)], they no longer cancel in the extrapolations (23) as they did in the single-histogram equations (12) and (13). Thus they need to be determined at least at the simulation points.

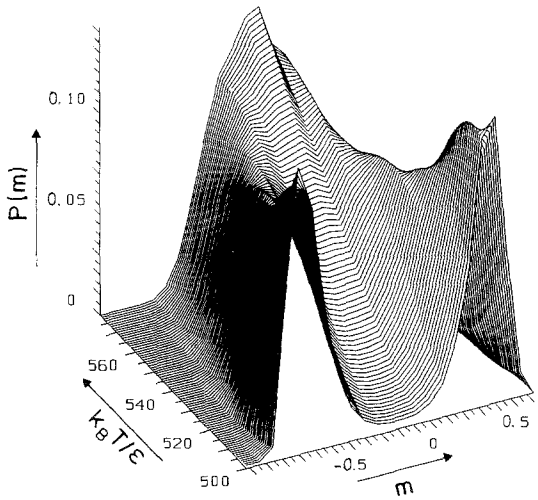

Fig. 5. Extrapolated order parameter distribution for $N = 256$ and $L = 112$ as a function of temperature in the critical region with $\Delta\mu = \Delta\mu_c = 0$. Note the symmetric double peak below T_c.

Note that the extrapolated expression for $\mathscr{Z}$ in Eqs. (23) inherits a self-consistency requirement if one choose for the parameters $(\beta', \Delta\mu')$ one of the simulation points. Explicitly,

$$\mathscr{Z}(N, \beta_k, \Delta\mu_k) = \int dM \int dE \frac{\sum_{i=1}^{s} (1+2\tau_i)^{-1} H^{\beta_i, \Delta\mu_i}(E, M)\, e^{\beta_k(\Delta\mu_k MN/2 - E)}}{\sum_{j=1}^{s} (1+2\tau_j)^{-1} [\mathscr{N}_j/\mathscr{Z}(N, \beta_j, \Delta\mu_j)]\, e^{\beta_j(\Delta\mu_j MN/2 - E)}} \quad \forall k \in \{1,..., s\} \qquad (27)$$

With a suitable set $\vec{\mathscr{Z}}^0 \equiv (\mathscr{Z}_1^0,..., \mathscr{Z}_s^0)$ of starting values this equation can be used as an iteration scheme to produce a self-consistent set of partition functions. Formally this iteration can be described with two (highly non-linear) operator $\vec{\mathbf{x}}$ and $\mathbf{y}$ (vector arrows are meant with respect to the "simulation index" $j = 1,..., s$),[36]

$$\vec{\mathscr{Z}}^{n+1} = \vec{\mathbf{x}}\mathbf{y}\vec{\mathscr{Z}}^n$$

where the action of the jth component of $\mathbf{x}$ on a function $h(E, M)$ is

$$\mathbf{x}_j h(E, M) := \int dM \int dE \sum_{i=1}^{s} e^{\beta_j(\Delta\mu_j MN/2 - E)} (1+2\tau_i)^{-1} H_{\beta_i, \Delta\mu_i}(E, M)/h(E, M)$$

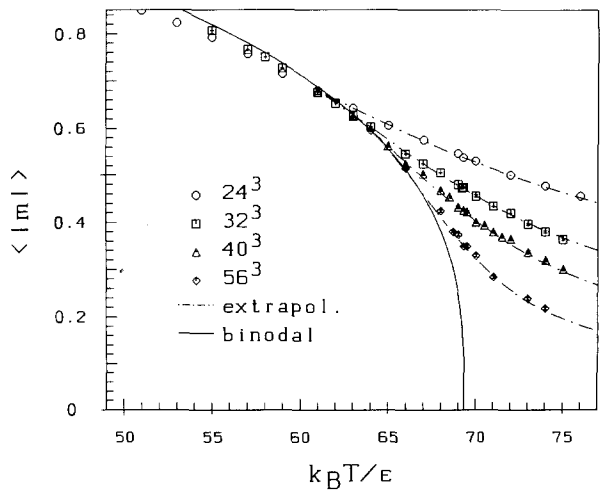

Fig.. 6. Order parameter (phase diagram) for mixtures with $N = 32$ and system sizes as indicated in the figure. Symbols denote averages measured during simulations, dash-dotted lines denote the histogram extrapolations. The full line is the binodal resulting from finite-size scaling.

and the action of $\mathbf{y}$ on a vector $\vec{g}$ is

$$\mathbf{y}\vec{g} := \sum_{j=1}^{s} e^{\beta_j(\Delta\mu_j MN/2 - E)}(1+2\tau_j)^{-1}\mathcal{N}_j/g_j$$

A set $\vec{\mathcal{Z}}^0$ of starting values which produced a very fast convergence of the iteration in all cases is $\mathcal{Z}_j^0 = \mathcal{N}_j$, motivated by Eq. (16). Then the self-consistent set of partition functions at the simulation points after n iteration is

$$\vec{\mathcal{Z}}^n = [\tilde{\mathbf{x}}\mathbf{y}]^n \vec{\mathcal{N}} \tag{28}$$

The convergence of the iteration was so fast that for all investigated systems after less than 100 steps the relative difference between two generations of partition functions fell from ≈ 1 to a value less than 10^{-10},

$$\left| \frac{\mathcal{Z}_k^n}{\mathcal{Z}_k^{n-1}} - 1 \right| < 10^{-10} \qquad \forall k \in \{1,\ldots, s\}$$

This criterion was used to stop the iteration.[36] Only *after* the partition functions have been determined in this way can the extrapolation equations (23) be used. Of course this procedure again can only produce the partition functions up to a common constant factor. But this undeterminable com-

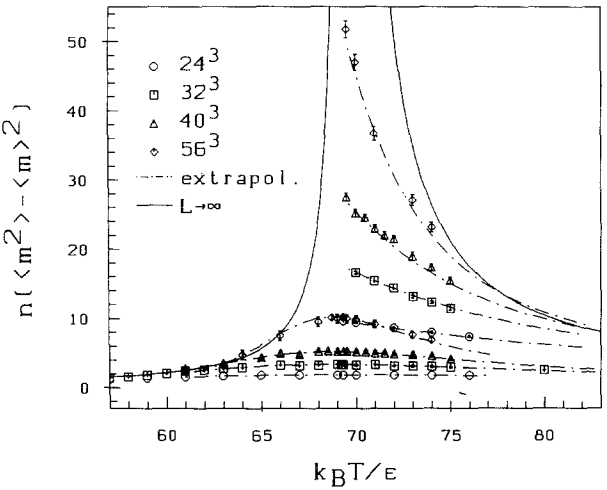

Fig. 7. Susceptibility for mixtures with $N = 32$ and system sizes as in Fig. 6. Again symbols denote measured averages and dash-dotted lines histogram extrapolations. The full lines are the $L \to \infty$ limit from finite-size scaling. Note that above T_c, $\langle m^2\rangle - \langle m\rangle^2$ is a factor of ≈ 2.8 larger than $\langle m^2\rangle - \langle |m|\rangle^2$, as discussed in the Appendix.

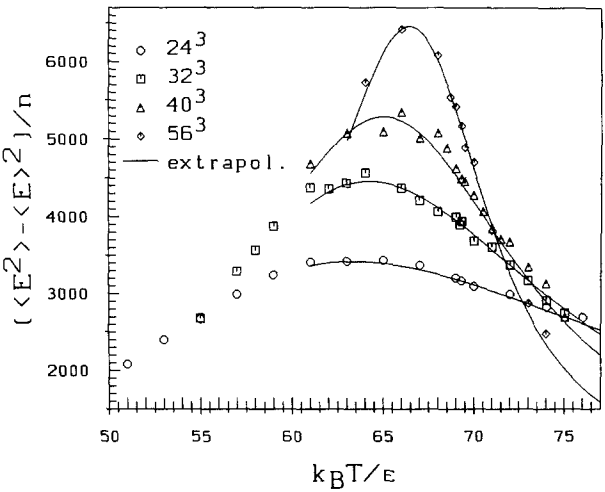

Fig. 8. Specific heat for mixtures with $N=32$ and system sizes as in Fig. 6. Again symbols denote measured averages and lines histogram extrapolations.

mon factor is irrelevant (i.e., cancels) in Eqs. (23) and again reflects the fact that the zero of the entropy cannot be obtained. Figures 6–7 and 9–11 show the order parameter, its susceptibility, and the specific heat as a function of temperature in the critical region for mixtures with chains of length $N=32$ and $N=128$, respectively. The plots of the order parameter along the temperature axis can be viewed as the phase diagrams of the

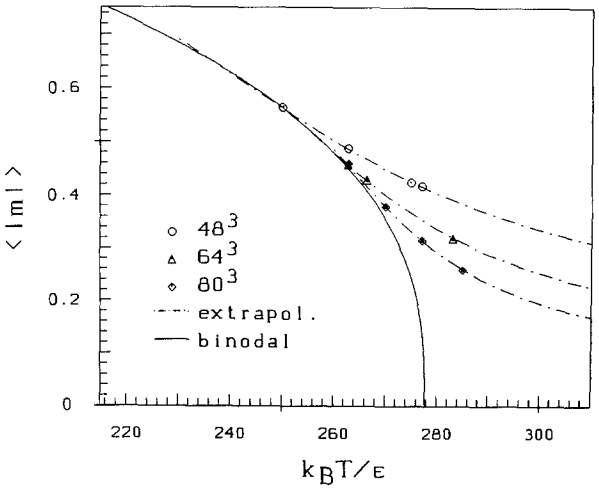

Fig. 9. As Fig. 6, but for chain length $N=128$.

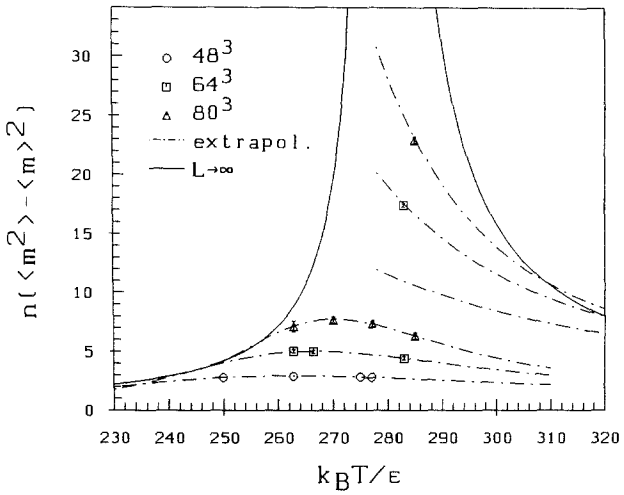

Fig. 10. As Fig. 7, but for chain length $N = 128$.

mixtures. Since the mixtures are fully symmetric, only the part for positive order parameter is shown [see Eq. (4)]. The binodal is obtained by the finite-size scaling methods described below; also the spinodal can be obtained by extrapolation of the inverse collective structure factor (making extensive use of the histogram methods) as described in refs. 44 and 36. Table I shows where and with how much statistics the histograms used for the extrapolations were obtained.

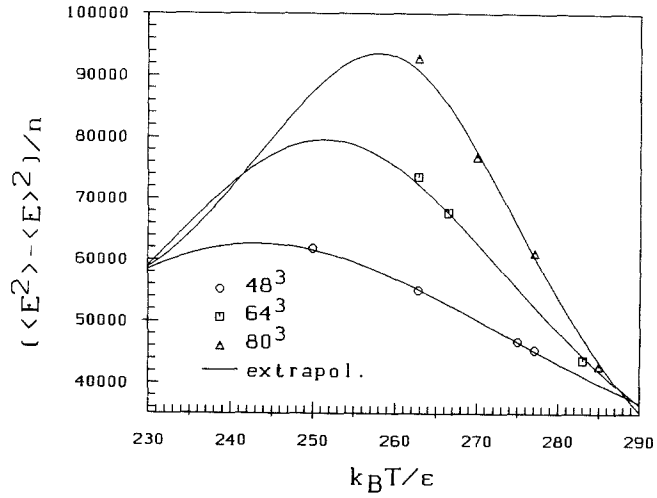

Fig. 11. As Fig. 8, but for chain length $N = 128$.

Table I. Simulation Points and Statistics

N	T	$\Delta\mu$	$\mathcal{N}$
32	69.3	0	22800
	68.7	0	13968
	68.7	0.281	13920
128	262.8	0	5520
	266.4	0	16800
	283.0	0	7920
	288.1	0	13200
	277.1	0.281	18360

As can be seen in the figures, for $N = 32$ many more simulations were done with only the conventional averages recorded and the extrapolations nicely go through all these data points. Therefore all the computer time for these additional runs could have been saved (and indeed has been saved for the longer chain lengths) because they do not give any more information than already contained in the few histograms of the above table. (But of course they still were necessary to judge the validity of the method).

Another example of what can be obtained from the histograms is shown in Fig. 12, which shows the equation of state $m(T, \Delta\mu)$ as a complete surface over the entire critical region for the mixture with $N = 256$. To obtain such a surface with conventional methods would require an extremely large simulational effort with many different simulation points.

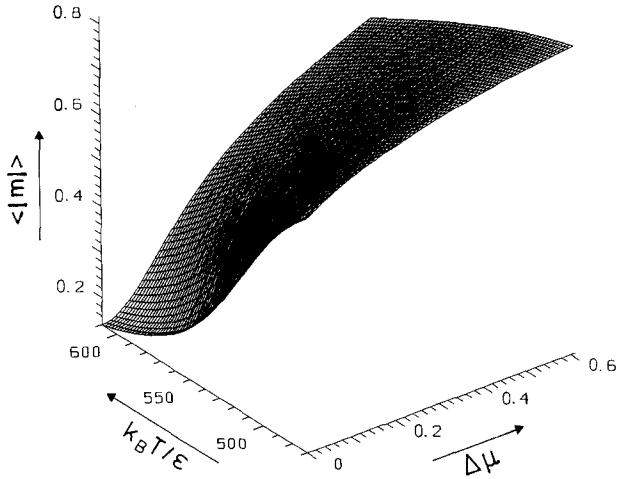

Fig. 12. Equation of state from multiple-hisogram extrapolations over the entire critical region for a mixture with $N = 256$ and $L = 112$.

3.5. Generalization to Asymmetric Mixtures

The generalization of the histogram methods to extrapolations other than in the direction of temperature and chemical potential (external field) is straightforward and will briefly be demonstrated for the case of polymer mixtures with *asymmetric* interaction potential.[36] Instead of Eq. (2), let us now consider the case

$$\varepsilon_{BB} = -\varepsilon_{AB} = -\varepsilon, \qquad \varepsilon_{AA} = -\lambda\varepsilon \tag{29}$$

Here $\lambda = \varepsilon_{AA}/\varepsilon_{BB}$ is called an asymmetry parameter. The internal energy in these systems is

$$E = -\varepsilon(\lambda n_{AA} + n_{BB} - n_{AB}) \tag{30}$$

where n_{IJ} denotes the number of interactions between monomers of species I and J. One can establish equations similar to (23) for extrapolations in the direction of λ as well as in the direction of β and $\Delta\mu$. Since one now has one more direction to extrapolate into, slightly more detailed histograms are necessary. As can be seen from Eq. (30), instead of recording histograms for M and E, one should now record histograms of $(M, n_{AA}, n_{BB}, n_{AB})$. Then extrapolations with respect to β, $\Delta\mu$, and λ are possible. The equations look *exactly* the same as Eqs. (23) except that instead of Eq. (24) the quantities $X(E, M)$ and $Y(E, M)$ now read

$$\begin{aligned} X(M, n_{AA}, n_{BB}, n_{AB}) &= \sum_{j=1}^{s} \frac{H_{\beta_j, \Delta\mu_j, \lambda_j}(M, n_{AA}, n_{BB}, n_{AB})}{1 + 2\tau_j} \\ Y(M, n_{AA}, n_{BB}, n_{AB}) &= \sum_{j=1}^{s} \frac{\mathcal{N}_j e^{\beta_j(\Delta\mu_j MN/2 + \varepsilon(\lambda_j n_{AA} + n_{BB} + n_{AB}))}}{(1 + 2\tau_j)\,\mathcal{Z}(N, \beta_j, \Delta\mu_j, \lambda_j)} \end{aligned} \tag{31}$$

and the integrations in Eqs. (23) are over those new arguments of X and Y. One need not worry that such high-dimensional histograms have very poor statistics in each entry—probably only zero or one event—because the extrapolation equations always *integrate* over all the entries of the histogram and therefore only the statistics of the whole histogram are relevant, but not the statistics of the individual entries. In fact it is wise to store the histograms as lists, i.e., to write down each pair (E, M) or each quadruple $(M, n_{AA}, n_{BB}, n_{AB})$ when it is measured, no matter whether it did occur before or not. In this way the amount of information to store is of the order of the number of measurements taken, whereas, if one would store true two- or four-dimensional histograms one would (especially for large systems, where M and E or the n_{IJ} have wide ranges) have to store huge arrays mostly containing zeros. Also, by storing the histograms as

lists one truly keeps the *complete* information generated by the simulations and avoids all systematic errors connected with dividing a histogram into bins.

4. FINITE-SIZE SCALING AT THE UNMIXING TRANSITION

4.1. General Aspects

A common practice in the physics of critical phenomena[45,46] is to expand the second derivatives of the free energy (which diverge at a second-order transition point) and certain first derivatives like the order parameter (which vanishes at the transition point) with respect to powers of the distance from the critical point,

$$g(t, \mu \equiv 0) = at^x(1 + bt^y + \cdots), \qquad y > 0 \tag{32a}$$

or

$$g(t \equiv 0, \mu) = a\mu^x(1 + b\mu^y + \cdots), \qquad y > 0 \tag{32b}$$

Here t and μ denote, respectively, the normalized distances of temperature T and chemical potential difference (per monomer) $\Delta\mu$ from their critical values T_c and $\Delta\mu_c$:

$$t := 1 - T/T_c, \qquad \mu := N(\Delta\mu - \Delta\mu_c)/k_B T \tag{33}$$

Note that μ is normalized *per chain* to make the analogy to a corresponding magnetic system as complete as possible. In Eq. (32) the prefactor a is called the critical amplitude and the exponent x the critical exponent of the quantity g. Since $y > 0$, it is clear that close to the critical point, in the so-called scaling region, g is completely described by its critical amplitude and its critical exponent. Therefore much effort has been devoted to the determination of the critical exponents (and amplitudes) of many statistical systems.[45,47] Common symbols have been established to denote the critical exponents for the order parameter m, its susceptibility χ, the correlation length of the order parameter fluctuations ξ, the specific heat C, and the pair correlation $G(r := |\vec{r} - \vec{r}|)$:

$$\begin{aligned} &C \sim t^{-\alpha}, \quad m \sim t^{\beta}, \quad \chi \sim t^{-\gamma}, \quad \xi \sim t^{-\nu}, && \text{for} \quad t \to 0, \quad \mu \equiv 0 \\ &m \sim \mu^{1/\delta}, \qquad \chi \sim \mu^{-\gamma/\beta\delta}, \quad \xi \sim \mu^{-\nu/\beta\delta}, && \text{for} \quad t \equiv 0, \quad \mu \to 0 \\ &\qquad\qquad G(r) \sim r^{-(d-2+\eta)} && \text{for} \quad t \equiv 0, \quad \mu \equiv 0 \end{aligned} \tag{34}$$

The exponents of χ and ξ along the critical isotherm ($t \equiv 0$, $\mu \to 0$) are

determined from $m \sim \mu^{1/\delta}$, $\chi \sim \partial m/\partial \mu$ with the help of the scaling relations[37,45]

$$\gamma = \nu(2-\eta), \qquad \delta = 1 + \gamma/\beta \tag{35}$$

These equations, which should hold for any system, do not contain the system dimension d. There is another set of equations, the so-called hyperscaling relations,[37,48,49] which do contain d and do not hold for every system (for instance, not for mean-field systems except at the marginal dimension $d=4$):

$$d\nu - 2\beta = \gamma \Leftrightarrow \alpha = 2 - d\nu \tag{36}$$

This has all been well known for many years and is only stated here to introduce the notation. Also well known is that many statistical systems can be put into only a few so-called universality classes[37,45] where the critical exponents are the same within each class. For instance, for the universality class of the 3D Ising model the exponents are[50]

$$\alpha = 0.113, \quad \beta = 0.324, \quad \gamma = 1.239, \quad \delta = 4.82, \quad \nu = 0.629, \quad \eta = 0.031 \tag{37}$$

Three-dimensional polymer mixtures of not too long chains very close to the critical point should belong to this universality class on theoretical grounds (mapping onto the corresponding Ising system, Ginzburg criterion) which by now is well established experimentally[17] as well as by Monte Carlo simulations.[18] But for long chains, $N \to \infty$, the Ginzburg criterion[13–16] also implies that the mixtures should display mean-field behavior, i.e.,

$$\alpha = 0, \quad \beta = 1/2, \quad \gamma = 1, \quad \delta = 3, \quad \nu = 1/2, \quad \eta = 0 \tag{38}$$

In this case hyperscaling (36) is not valid.

Now all the singularities of the second free energy derivatives at the critical point can be traced down to stem from a diverging characteristic length of the system. This characteristic thermodynamic length l in general[51–53] diverges like

$$l \sim t^{-(\gamma+2\beta)/d} \tag{39}$$

and becomes the correlation length ξ if hyperscaling is valid. Since in the finite systems accessible by computer simulations there cannot exist a length larger than the system size L, the finite size of the systems will obscure the physics as soon as the system is so close to the critical point that its characteristic length starts to exceed L, i.e., as soon as $l > L$ (or

$\xi > L$ in the hyperscaling case). Therefore no true singularities can be measured and the susceptibilities in Figs. 7 and 10 show the familiar finite-size rounding and the order parameter in Figs. 6 and 9 the finite-size tails near T_c. These effects are well understood and can be taken into account by the finite-size scaling theory[54–57] which (for systems of hypercubic shape[51,57]) can be summarized in a very general and complete form by two equations for the size dependence of the free energy per particle F and the correlation length ξ:

$$F(L, t, \mu) = L^{-d}\tilde{F}(L^u t, L^{d-v}\mu), \qquad \xi(L, t, \mu) = L\tilde{\xi}(L^u t, L^{d-v}\mu) \quad (40)$$

with the abbreviations

$$u := \frac{d}{\gamma + 2\beta} = \begin{cases} 1/\nu \\ d/2 \end{cases} \qquad v := \frac{\beta d}{\gamma + 2\beta} = \begin{cases} \beta/\nu & \text{hyperscaling} \\ d/4 & \text{mean field} \end{cases} \quad (41)$$

$\Rightarrow$

$$\alpha = 2 - \frac{d}{u}, \qquad \beta = \frac{v}{u}, \qquad \gamma = \frac{d-2v}{u}, \qquad \delta = \frac{d}{v} - 1, \quad \text{etc.} \quad (42)$$

In Eq. (40) and in the following a tilde denotes a size-independent function of the arguments. This general scaling form of the free energy determines completely the finite-size scaling of any moment of the order parameter or the internal energy, which are just derivatives of the free energy.

A more pedestrian derivation of finite-size scaling starts with an ansatz for the order parameter distribution $P_{t,\mu}(m)$ allowing explicit and implicit L dependence of P through all its variables, i.e., $P = P(t(L), \mu(L), m(L), L)$. The basic scaling assumption that the thermodynamic length l, Eq. (39), is the relevant length scale in the system, i.e.,that L has to be measured in units of l, the normalization condition $\int dm\, P(m) = 1$, and the requirement that near the critical point the power laws (34) for the moments of the order parameter have to be reproduced by its distribution, lead[36] to the finite-size scaling form

$$P(t(L), \mu(L), m(L), L) = L^v \tilde{P}(L^u t, L^{d-v}\mu, L^v m) \quad (43)$$

Figures 13 and 14 show this scaling behavior for the order parameter distribution of mixtures with chain length $N = 32$ and $N = 64$, respectively. For $N = 64$ the (effective) exponents are no longer Ising (see Table II), but the scaling form (43) is of course still valid. From this distribution the scaling of the moments follows directly,

$$\langle m^k \rangle_L = L^{-kv}\tilde{m}_k(L^u t, L^{d-v}\mu) \quad (44)$$

with scaling functions $\tilde{m}_k = \int dx\, x^k \tilde{P}(L^u t, L^{d-v}\mu, x)$. As the scaling form

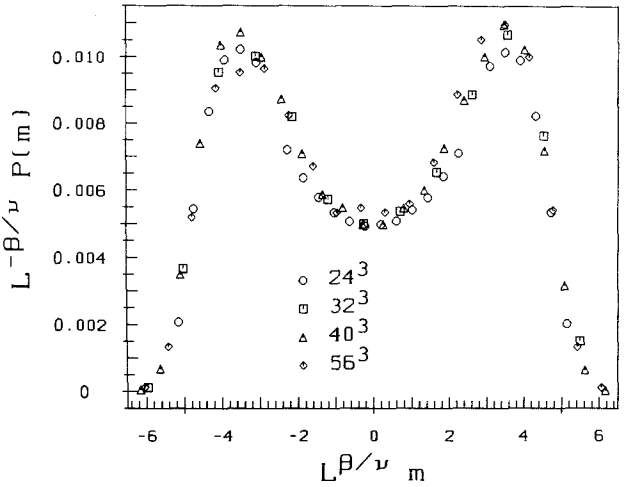

Fig. 13. Scaled order parameter distribution at the critical point for mixtures with $N=32$ and system sizes as indicated in the figure. For this plot the extrapolated distributions were binned to eliminate the noise.

(40), this general scaling is valid with and without hyperscaling. Incorporating hyperscaling (36) and using Eqs. (42) and (35), one arrives at the more familiar form

$$\langle m^k \rangle_L = L^{-k\beta/\nu} \tilde{f}_k(L^{1/\nu}t, L^{\delta\beta/\nu}\mu)$$
$$\langle m^k \rangle_L = L^{-k(d-2+\eta)/2} \tilde{f}_k(L^{-1}\xi, L^{(d-2+\eta)\delta/2}\mu) \tag{45}$$

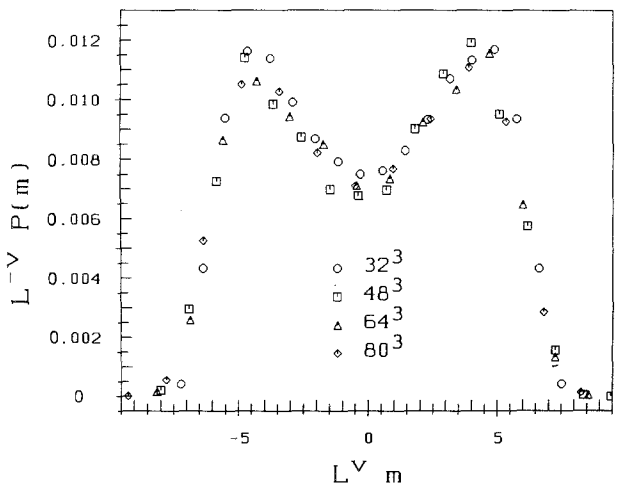

Fig. 14. As Fig. 13, but for chain length $N=64$, and system sizes as indicated in the figure.

Table II. Critical Temperatures, Exponents, and Amplitudes

N	$k_B T_c/\varepsilon$	u	v	C_m^t	C_m^μ	C_χ^t	C_χ^{-t}	C_χ^μ	C_χ^m
Ising		$1/\nu = 1.59$	$\beta/\nu = 0.51$						
16	36.15 ± 0.20	1.56 ± 0.03	0.50 ± 0.02	1.38	0.995	0.20	0.96	0.40	0.59
32	69.35 ± 0.30	1.59 ± 0.03	0.505 ± 0.02	1.36	0.98	0.18	0.86	0.37	0.57
64	138.9 ± 0.2	1.53 ± 0.03	0.565 ± 0.02	1.39	0.964	0.24	0.82	0.43	0.56
128	277.7 ± 0.6	1.58 ± 0.04	0.561 ± 0.03	1.29	0.956	0.27	0.72	0.45	0.50
256	540.6 ± 10	1.53 ± 0.04	0.623 ± 0.04	1.51	1.03	0.25	0.85	0.49	0.76
Mean field		$d/2 = 1.5$	$d/4 = 0.75$						

In the second equation I eliminated t in favor of the correlation length ξ [see Eq. (34)]. Comparing the explicit L dependences in the prefactors of these scaling forms, one immediately recognizes hyperscaling. These forms are valid for the limiting behavior of the polymer mixtures with short chains, namely in the Ising limit (37). The scaling forms in the long-chain limit follow from Eqs. (44) and (38) yielding the mean-field finite-size scaling

$$\langle m^k \rangle_L = L^{-kd/4} \tilde{m}_k(L^{d/2} t, L^{3d/4} \mu) \tag{46}$$

At this point I should mention that for polymer systems one has to be very careful in chosing the scaling variables. In fact, if the chain length N is not held fixed, then L is *not* the right scaling variable because it is not uniquely related to the number of degrees of freedom involved in the phase transition. Then the number of chains (number of spins in the corresponding magnetic system) $n \sim L^d/N$ rather than L is the right scaling variable and one should replace L by $LN^{-1/d}$ in all scaling forms. This subtlety need not be considered if N is a fixed parameter as in spin systems, where one could say $N \equiv 1$, or in the analysis presented here, where finite-size scaling is considered for each chain length *separately*, but it becomes relevant in the recently derived[44,36] crossover finite-size scaling equations, where L and N are allowed to vary simultaneously.

4.2. Ratios of Moments

Equation (44) implies that there is no explicit size dependence in ratios of the form

$$U_{ij}^{lk}(L, t, \mu) = \frac{\langle m^l \rangle_L^k}{\langle m^i \rangle_L^j} = \frac{\tilde{m}_l(L^u t, L^{d-v}\mu)^k}{\tilde{m}_i(L^u t, L^{d-v}\mu)^j} \qquad \text{with} \quad lk = ij \tag{47}$$

because the prefactors cancel. The only L dependence left in these ratios is implicit via the variables of the scaling function $\tilde{m}_k$. Right at the critical point where $(t, \mu) = (0, 0)$ there is no L dependent left at all (apart from corrections to scaling, which currently cannot be resolved in polymer mixtures, however) and the $U_{ij}^{lk}(L, t, \mu)$ for different L should coincide at this point. The intersection of $U_{ij}^{lk}(L, T, \Delta\mu \equiv \Delta\mu_c)$ with different L then yields T_c. This is nicely demonstrated in Figs. 15 and 16. I used the ratios involving the smallest possible moments, since they have the best statistics,

$$U_{12}^{21}(L, t, \mu) = \frac{\langle m^2 \rangle_L}{\langle |m| \rangle_L^2} \tag{48}$$

Note that there is the estimator for the absolute value $\langle |m| \rangle$ in the denominator and not just $\langle m \rangle$. This is necessary for all odd-order parameter moments to obtain sensible results in the thermodynamic limit as discussed in detail in the Appendix. Note that this determination of T_c is independent of the critical exponents.

Another ratio out of the family (47) has previously been used in the literature to determine T_c, namely Binder's cumulant or renormalized coupling constant,[58] which corresponds to U_{22}^{41}. This has the disadvantage that it needs moments up to fourth order, but since it involves only even moments, one need not worry about using absolute values.

While the ratio (47) was constructed to eliminate the explicit L

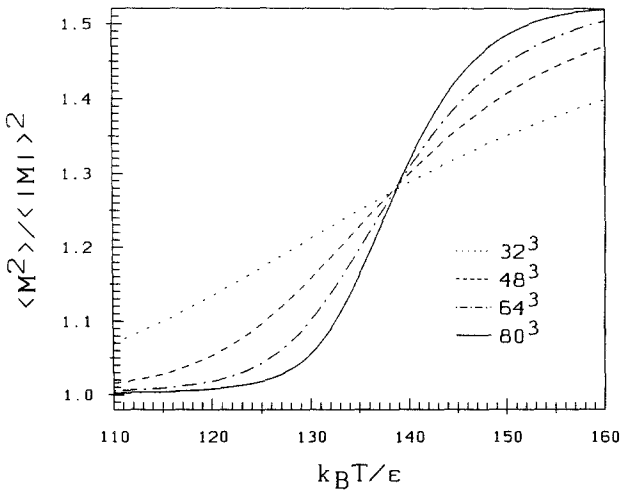

Fig. 15. U_{12}^{21} as a function of temperature with $\mu \equiv 0$ for chain length $N = 64$ and system sizes as indicated in the figure. Note the sharply located intersection point yielding T_c and U^*.

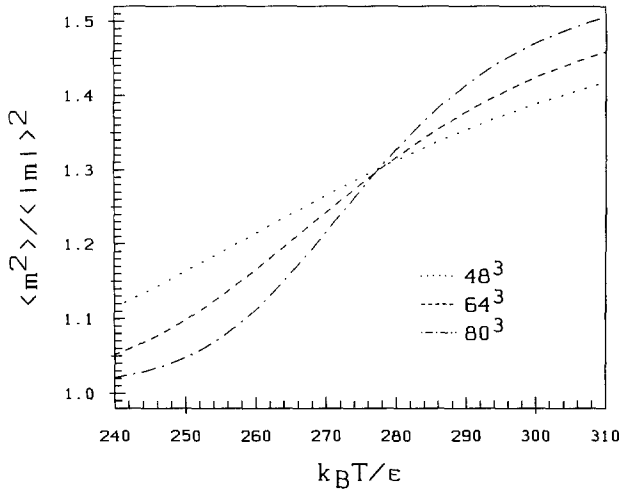

Fig. 16. U_{12}^{21} as a function of temperature with $\mu \equiv 0$ for chain length $N = 128$ and system sizes as indicated in the figure.

dependence from Eq. (44), one can on the contrary use this L dependence to determine the exponent v by constructing ratios of the form

$$W_k(L_2, L_1, t, \mu) := -\ln\left(\frac{\langle m^k\rangle_{L_2}}{\langle m^k\rangle_{L_1}}\right)\Big/\ln\left(\frac{L_2}{L_1}\right)$$

$$= kv - \ln\left(\frac{\tilde{m}_k(L_2^u t, L_2^{d-v}\mu)}{\tilde{m}_k(L_1^u t, L_1^{d-v}\mu)}\right)\Big/\ln\left(\frac{L_2}{L_1}\right) \qquad (49)$$

At the critical point $(t, \mu) = (0, 0)$ the scaling functions $\tilde{m}_k$ are both equal to $\tilde{m}_k(0, 0)$ and W_k becomes $W_k(L_2, L_1, 0, 0) = kv$, yielding directly the exponent v. Again for best possible accuracy I use the ratio involving the smallest moments and since these are odd moments the absolute value of the order parameter is needed (see the Appendix):

$$W_1(L_2, L_1, t, \mu) = -\ln\left(\frac{\langle|m|\rangle_{L_2}}{\langle|m|\rangle_{L_1}}\right)\Big/\ln\left(\frac{L_2}{L_1}\right) \qquad (50)$$

In Fig. 18 this function is shown for the mixture with $N = 64$. For this chain length $W_1(T_c)$ already lies above the Ising value but is still far away from mean field. The crossover from Ising to mean field is discussed in detail in refs. 44 and 36.

Now one critical exponent is not enough. To determine the whole set, at least one more is needed. Since the explicit L dependence in Eq. (44)

only provides v, the only chance to obtain another exponent is the *implicit* L dependence of $\tilde{m}_k$ in Eq. (44). This implicit dependence can be made explicit by a Taylor expansion around the critical point. A suitable function for this again is provided by the ratios in Eq. (47),

$$U(L^u t, L^{d-v}\mu) \approx \underbrace{U(0,0)}_{U^*} + \underbrace{L^u t \left.\frac{\partial U}{\partial (L^u t)}\right|_{t=0,\mu=0}}_{A} + \underbrace{L^{d-v}\mu \left.\frac{\partial U}{\partial (L^{d-v}\mu)}\right|_{t=0,\mu=0}}_{B} + \cdots \tag{51}$$

To simplify the notation, the indices i, j, k, l of U are omitted here. Since by construction U is not explicitly L dependent, the value of U at $(0, 0)$ and all its derivatives at $(0, 0)$ are completely independent of L, so that the only size dependences up to first order are the ones explicitly shown above. Now if among the family of ratios (47) there exists a function U which is sufficiently linear near the critical point, then the exponents of the scaling variables $L^u t$ and $L^{d-v}\mu$ can be measured by considering $U(L_2)$ as a function of $U(L_1)$. The derivative of this new function up to first order yields

$$\left.\frac{dU(L_2, L^u t, 0)}{dU(L_1, L^u t, 0)}\right|_{U^*} \approx \frac{U(L_2, L^u t, 0) - U^*}{U(L_1, L^u t, 0) - U^*} \sim \left(\frac{L_2}{L_1}\right)^u \qquad \text{for} \quad \mu \equiv 0 \tag{52}$$

$$\left.\frac{dU(L_2, 0, L^{d-v})}{dU(L_1, 0, L^{d-v})}\right|_{U^*} \approx \frac{U(L_2, 0, L^{d-v}) - U^*}{U(L_1, 0, L^{d-v}) - U^*} \sim \left(\frac{L_2}{L_1}\right)^{d-v} \qquad \text{for} \quad t \equiv 0 \tag{53}$$

In the first step the differential was approximated by the difference quotient, in the second step the Taylor expansion was used. Figure 17 shows the ratios $U_{12}^{21}(L, t, \mu \equiv 0)$ as functions of each other. They intersect each other at $U^* = U_{12}^{21}(0, 0)$, where they are sufficiently linear. The exponent u can be determined from the slope of these functions at U^*, i.e., by fitting straight lines to the functions at U^*. It can already be seen from Figs. 15 and 16 that the ratios U_{12}^{21} are sufficiently linear to apply the above method.

Since these functions are linear over a quite large range around U^* (i.e., around T_c), the exponents determined in this way are not as sensitive to errors in T_c as are the exponents determined with W_k, Eq. (49). On the other hand, there are more approximations involved like the Taylor expansion, the difference quotient instead of the differential, and the fitting of straight lines to the functions as U^*. Altogether it is hard to say which method is more accurate and certainly other systems than polymers

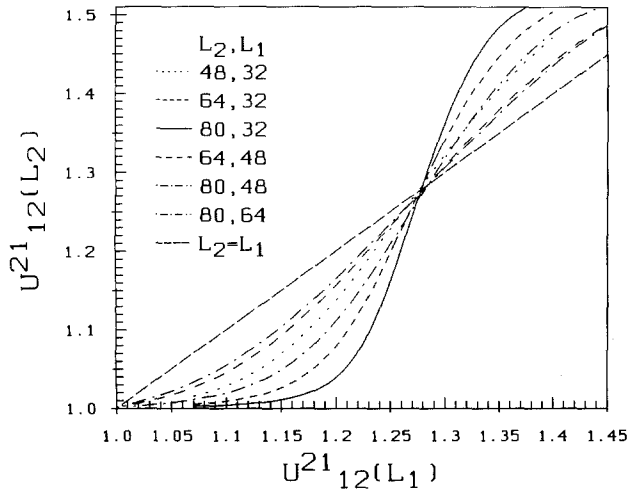

Fig. 17. U_{12}^{21} from Fig. 15 as a function of each other; relations of system sizes as indicated in the figure.

are much more suitable for high-precision measurements of critical exponents.[59]

Of course the measured exponents for the long chains which are not Ising nor mean field are to be understood as only effective exponents resulting from the system crossover from Ising to mean field as is discussed in detail in refs. 44 and 36.

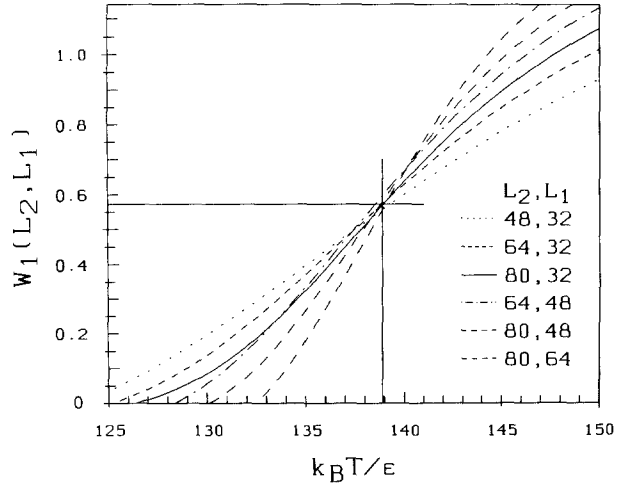

Fig. 18. W_1 for the same system as in Fig. 15. The values of W_1 at T_c yield the exponent ν as shown.

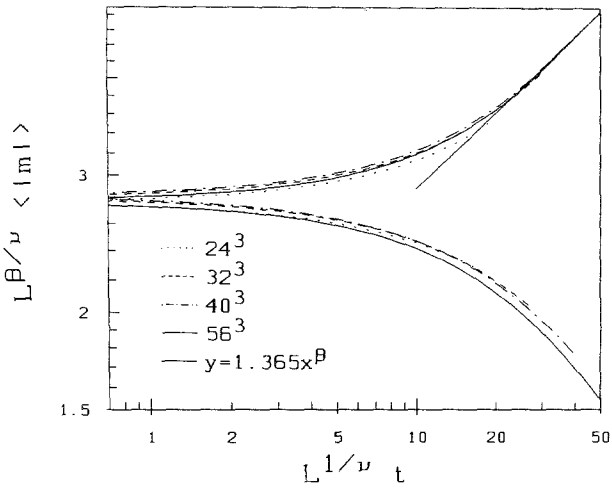

Fig. 19. Ising-scaled order parameter along the temperature axis for the mixture with $N=32$, system sizes as in Fig. 6, meaning of lines as indicated in the figure.

The critical exponents and temperatures obtained with this analysis can be checked in so-called finite-size scaling plots where the scales of the axes are chosen such that the curves for different L collapse on one master curve if the exponents (and T_c) used are right. Figures 19–24 show such plots for mixtures of chains with $N=32$ (which still belong to the Ising limit) and with $N=128$ (which are significantly off the Ising limit). The

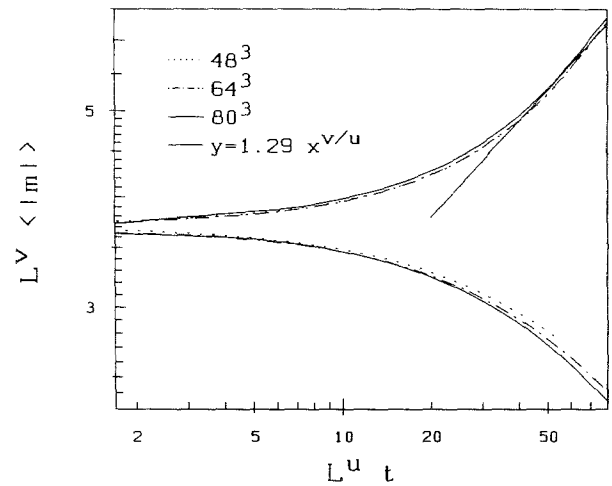

Fig. 20. Scaled order parameter along the temperature axis for the mixture with $N=128$, system sizes as in Fig. 9, meaning of lines as indicated in the figure.

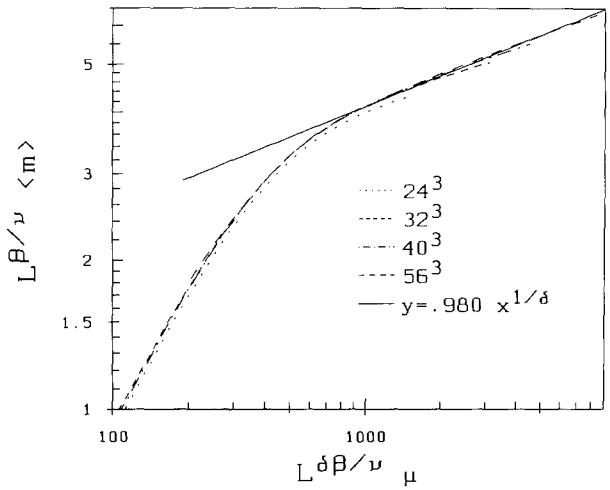

Fig. 21. Ising-scaled order parameter along the critical isotherm for the mixture with $N = 32$, system sizes as in Fig. 6, meaning of lines as indicated in the figure.

scales of the axes follow from Eq. (44), which for the order parameter $\langle |m| \rangle$ and its susceptibility $k_B T\chi = L^d(\langle m^2 \rangle - \langle m \rangle^2)$ read

$$L^v \langle |m| \rangle = \tilde{m}(L^u t, L^{d-v}\mu), \qquad L^{2v-d} k_B T\chi = \tilde{\chi}(L^u t, L^{d-v}\mu) \tag{54}$$

In the Ising regime, where hyperscaling is valid, this can be written as

$$L^{\beta/\nu} \langle |m| \rangle = \tilde{m}(L^{1/\nu} t, L^{\delta\beta/\nu}\mu), \qquad L^{-\gamma/\nu} k_B T\chi = \tilde{\chi}(L^{1/\nu} t, L^{\delta\beta/\nu}\mu) \tag{55}$$

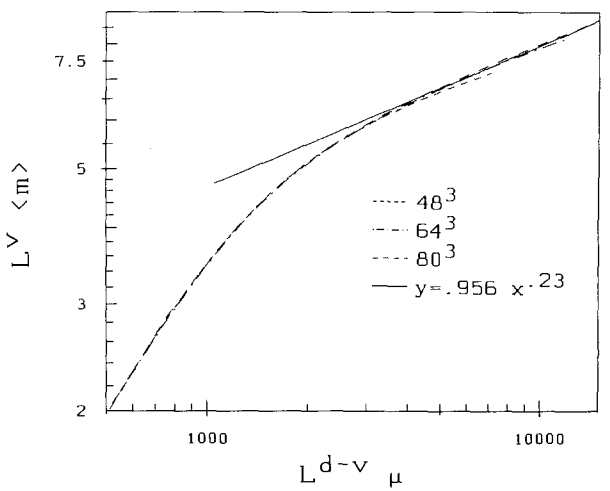

Fig. 22. Scaled order parameter along the critical isotherm for the mixture with $N = 128$, system sizes as in Fig. 9, meaning of lines as indicated in the figure.

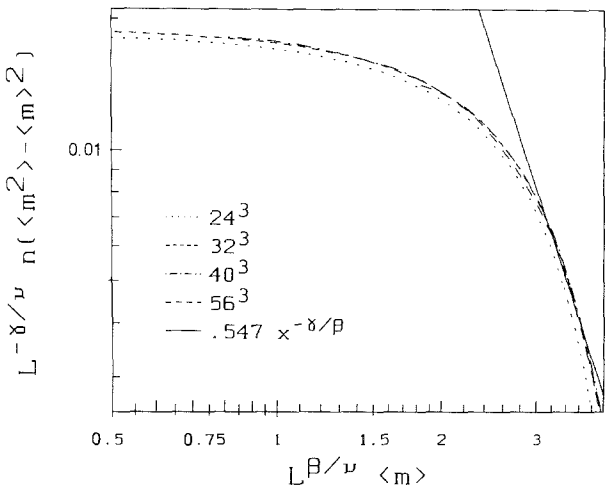

Fig. 23. Scaled susceptibility as a function of the order parameter for the mixture with $N = 32$, system sizes as in Fig. 6, meaning of lines as indicated in the figure.

Here I also show the scaling of χ as a function of m instead of μ, which should be measurable experimentally. This scaling follows easily from the above equations and reads

$$k_B T \chi_L = L^{d-2\nu} \tilde{\chi}(L^{\nu} m_L) = \begin{cases} L^{\gamma/\nu} \tilde{\chi}(L^{\beta/\nu} m_L) & \text{Ising} \\ L^{d/2} \tilde{\chi}(L^{d/4} m_L) & \text{mean field} \end{cases} \tag{56}$$

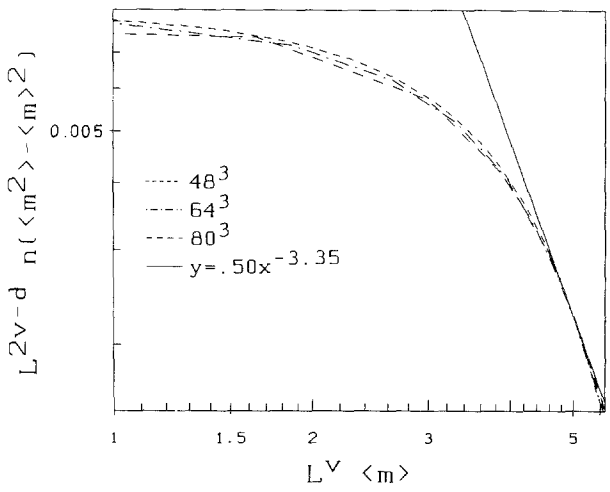

Fig. 24. Scaled susceptibility as a function of the order parameter for the mixture with $N = 128$, system sizes as in Fig. 9, meaning of lines as indicated in the figure.

Similar scaling plots along the temperature axis can also be found for short chains in ref. 18, while to my knowledge the finite-size scaling of polymer mixtures along the critical isotherm and as a function of m was not investigated earlier.

The scaling plots also yield the critical amplitudes if part of the so-called asymptotic regime lies within the scaling region, i.e., within the region where Eq. (34) or (44) is valid. This is the case for large enough L. The asymptotic regime of an L-dependent quantity g is the region which is far enough away from the critical point such that the value of g coincides with the values of g measured at larger systems, i.e., the set

$$\{T, \Delta\mu \mid g_L(T, \Delta\mu) = g_{L'}(T, \Delta\mu)\ \forall L' > L\}$$

For instance, if Figs. 6–9 a little below T_c the curves with different L merge together. For large L this region is still within the scaling regime and the scaling function $\tilde{m}(x = L^u t, 0)$ in Eq. (54) has to be $\sim x^\beta$, β in general from Eq. (42), to compensate the L dependence. Since $\tilde{m}$ is a scaling function, the proportionality constant C_m^t is independent of L. In the asymptotic regime the scaling forms (54) and (55) for the order parameter then simply are

$$\langle |m| \rangle = C_m^t t^\beta \tag{57}$$

and the constant C_m^t is the critical amplitude of the order parameter along the temperature axis. Therefore in the logarithmic plots of Figs. 19 and 20 the curves in the asymptotic regime merge to a straight line with slope β and offset C_m^t.

Similar considerations also hold along the critical isotherm yielding the amplitude C_m^μ from Figs. 21 and 22, and from Figs. 23, etc., one gets the critical amplitudes for the susceptibility. This method to measure critical amplitudes from finite-size scaling plots is standard and has been applied to many systems. It is well known that the errors involved are rather large, especially if (as in the case here for long chains) the errors of the exponents are already large. Usually one "knows" the exponents already because the system belongs to a known universality class (as is the case here for short chains). For long chains, however, the errors induced by the measured effective exponents are magnified to a great extent in the errors of the effective critical amplitudes. Nevertheless the critical amplitudes, exponents, and temperatures obtained with this analysis provided a rather satisfying picture of the $L \to \infty$ behavior of the investigated polymer mixtures. See, for instance, the phase diagrams in Figs. 6 and 9, where the binodal is just the asymptotic limit $m = C_m^t t^\beta$ of the order parameter; or the $L \to \infty$ limit

of the susceptibilities in Figs. 7 and 10. For the susceptibilities the critical amplitudes below and above T_c are different and there is an additional subtlety in the question of where to use $\langle |m| \rangle$ or $\langle m \rangle$ (see the Appendix).

4.3. Derivatives of ln $\mathscr{Z}$

From the correspondence between the (almost) grand canonical ensemble (8) of our polymer mixture and the canonical spin system it is clear that $\ln(\mathscr{Z})$ with the $\mathscr{Z}$ of Eq. (8) has a similar scaling form like F in Eq. (40). Since $\mathscr{Z}$ in Eq. (8) is the partition function of the whole system (not per particle) the correspondence is $-k_B T \ln \mathscr{Z} \hat{=} L^d F$. The finite factor $k_B T$ does not influence the scaling behavior, so that the finite-size scaling of $\ln \mathscr{Z}$ becomes

$$\ln \mathscr{Z} = \tilde{Z}(L^u t, L^{d-v}\mu) \tag{58}$$

For scaling considerations of $\ln \mathscr{Z}$ it is convenient to change the set of parameters $(\beta, \Delta\mu)$ in the partition function (8) to a set (β, κ) with the new parameter

$$\kappa \equiv \frac{N}{k_B T} \Delta\mu$$

This is only a modification with finite quantities of the parameter describing the chemical potential and does not affect the scaling behavior. Just use $\mu = 2(\kappa - \kappa_c)$ instead of Eq. (33). Like $(\beta, \Delta\mu)$, the set (β, κ) can be treated as independent parameters. The partition function (8) then simply reads

$$\mathscr{Z}(N, \beta, \kappa) = \int_n^n dM \int dE\, e^{\kappa M} e^{-\beta E} \Gamma(E, M) \tag{59}$$

Equations (58) and (59) are the two basic equations from which the finite-size scaling of a variety of moments and cross correlations of energy and order parameter follows. The relations between the derivatives $(\partial/\partial t, \partial/\partial\mu)$, which applied to Eq. (58) yield the scaling, and the derivatives $(\partial/\partial\beta, \partial/\partial\kappa)$, which applied to Eq. (59) yield the moments, involve only finite factors,

$$\frac{\partial}{\partial t} = k_B T_c \beta^2 \frac{\partial}{\partial \beta}, \qquad \frac{\partial}{\partial \mu} = \frac{1}{2} \frac{\partial}{\partial \kappa}$$

Therefore it does not affect the scaling if the one or the other set is used. For instance, for the first derivatives of $\ln \mathscr{Z}$ one gets

$$\begin{aligned} L^u \tilde{g}(L^u t, L^{d-v}\mu) &= \frac{\partial}{\partial t} \ln \mathscr{Z} \sim \frac{\partial}{\partial \beta} \ln \mathscr{Z} = -\langle E \rangle \\ L^{d-v} \tilde{g}(L^u t, L^{d-v}\mu) &= \frac{\partial}{\partial \mu} \ln \mathscr{Z} \sim \frac{\partial}{\partial \kappa} \ln \mathscr{Z} = \langle M \rangle \end{aligned} \tag{60}$$

Here the symbol $\sim$ means *has the same scaling behavior as* and $\tilde{g}$ denotes the appropriate scaling functions (I do not bother to write a different symbol for each scaling function). The last equation is of course consistent with Eq. (54); observe that M denotes the extensive order parameter, $M \sim L^d m$.

Similarly, one obtains for the finite-size scaling of the second derivatives

$$\begin{aligned} L^{2u} \tilde{g}(L^u t, L^{d-v}\mu) &\sim \frac{\partial^2}{\partial \beta^2} \ln \mathscr{Z} = \langle E^2 \rangle - \langle E \rangle^2 \sim L^d C \\ L^{2d-2v} \tilde{g}(L^u t, L^{d-v}\mu) &\sim \frac{\partial^2}{\partial \kappa^2} \ln \mathscr{Z} = \langle M^2 \rangle - \langle M \rangle^2 \sim L^d \chi \\ L^{d+u-v} \tilde{g}(L^u t, L^{d-v}\mu) &\sim \frac{\partial}{\partial \beta} \frac{\partial}{\partial \kappa} \ln \mathscr{Z} = \langle ME \rangle - \langle M \rangle \langle E \rangle \end{aligned} \tag{61}$$

In this way different exponent combinations appear in the *explicit* L dependence (prefactors of the $\tilde{g}$), which then are easily measurable as described below. Still other combinations, namely precisely the ones of the implicit L dependences of the scaled variables in the $\tilde{g}$, can be made explicit by considering *logarithmic* derivatives of $\ln \mathscr{Z}$:

$$\begin{aligned} L^u \tilde{g}(L^u t, L^{d-v}\mu) &\sim \frac{\partial}{\partial \beta} \ln \frac{\partial}{\partial \beta} \ln \mathscr{Z} = -\frac{\langle E^2 \rangle}{\langle E \rangle} + \langle E \rangle \\ &\sim \frac{\partial}{\partial \beta} \ln \frac{\partial}{\partial \kappa} \ln \mathscr{Z} = -\frac{\langle EM \rangle}{\langle M \rangle} + \langle E \rangle \\ L^{d-v} \tilde{g}(L^u t, L^{d-v}\mu) &\sim \frac{\partial}{\partial \kappa} \ln \frac{\partial}{\partial \kappa} \ln \mathscr{Z} = \frac{\langle M^2 \rangle}{\langle M \rangle} - \langle M \rangle \\ &\sim \frac{\partial}{\partial \kappa} \ln \frac{\partial}{\partial \beta} \ln \mathscr{Z} = \frac{\langle EM \rangle}{\langle E \rangle} - \langle M \rangle \end{aligned} \tag{62}$$

The exponent of the explicit L dependences of such functions can be

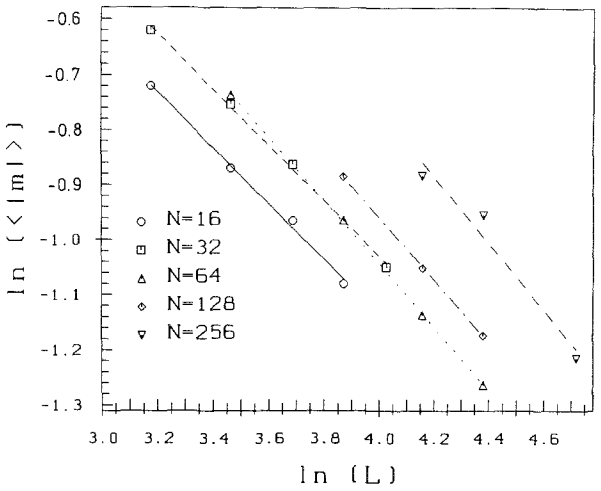

Fig. 25. Order parameter at the critical point as a function of system size L for all chain lengths N as indicated in the figure.

measured by evaluating those functions at *fixed* arguments ($x = L^u t$, $y = L^{d-v}\mu$) of $\tilde{g}$. Since $\tilde{g}$ is an L-independent scaling form, $\tilde{g}(x, y)$ is just a constant if evaluated at some fixed arguments (x_0, y_0) Therefore a log–log plot of the right-hand side of the above equations for different L but fixed scaling arguments (x_0, y_0) versus L should show a straight line with a slope equal to the exponent of the explicit L dependence on the corresponding left-hand side. This is demonstrated in Figs. 25 and 26, where the

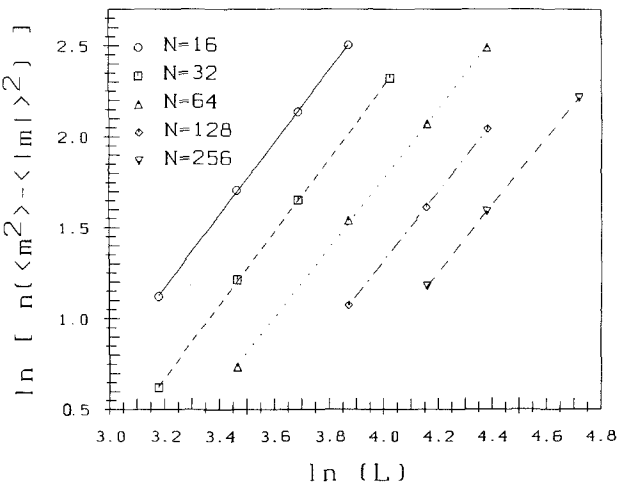

Fig. 26. Maximum of the susceptibility $(n\langle m^2\rangle - n\langle|m|\rangle^2)$ as a function of system size L for all chain lengths N as indicated in the figure.

magnetization at the critical point, i.e., at constant scaling variables $(x_0, y_0) = (0, 0)$ and the maximal susceptibility, i.e., the susceptibility at constant $(x_0, y_0) = (x^*, y^*)$, where the corresponding scaling function $\tilde{g}$ has its maximum, are plotted versus L. Observe that in principle it is better to use a function at its extremum instead at the critical point because then the obtained exponent is *independent* of the determination of T_c. That is why I presented so many possibilities to extract the exponents. The strategy then is to find suitable functions which have extrema within the scaling region and to extract the exponents from the values of these functions at their extrema. The necessity for the logarithmic derivatives, Eqs. (62), then results because they are the only functions which provide the *pure* inner exponents and still may have an extremum inside the scaling region. This gets clear when hyperscaling is valid. Then Eqs. (61) and (62) become

$$\begin{aligned} L^{d+\gamma/\nu}\tilde{g} &\sim \langle M^2\rangle - \langle M\rangle^2 \\ L^{d+\alpha/\nu}\tilde{g} &\sim \langle E^2\rangle - \langle E\rangle^2 \\ L^{d+(1-\beta)/\nu}\tilde{g} &\sim \langle ME\rangle - \langle M\rangle\langle E\rangle \qquad (63) \\ L^{1/\nu}\tilde{g} &\sim \langle E\rangle - \langle EM\rangle/\langle M\rangle \sim \langle E\rangle - \langle E^2\rangle/\langle E\rangle \\ L^{\delta\beta/\nu}\tilde{g} &\sim -\langle E\rangle + \langle EM\rangle/\langle E\rangle \sim -\langle M\rangle + \langle M^2\rangle/\langle M\rangle \qquad (64) \end{aligned}$$

In this picture the logarithmic derivative in the second from last line is the only way to extract ν disentangled from any other exponent.

Along the same lines one can of course construct many other functions, such as

$$\frac{\partial^{k+l}}{\partial\beta^k\,\partial\kappa^l}\ln\mathscr{Z} \qquad \text{and} \qquad \frac{\partial^k}{\partial\beta^k}\ln\frac{\partial^l}{\partial\kappa^l}\ln\mathscr{Z}$$

In fact, some of these, such as

$$\frac{\partial^2}{\partial\beta\,\partial\kappa}\ln\mathscr{Z} \sim \frac{\partial}{\partial\beta}\langle M\rangle \qquad \text{or} \qquad \frac{\partial^3}{\partial\beta^2\,\partial\kappa}\ln\mathscr{Z} \sim \frac{\partial^2}{\partial\beta^2}\langle M\rangle$$

have been used in recent high-precision simulations of the 3D Ising model.[59]

5. CONCLUSIONS

In this work I outlined a complete description of how to get information about the critical behavior of polymer mixtures by computer experiments, which because of the fundamental difficulties (a)–(c) men-

tioned in the Introduction has up to now not been performed for long chains. While with the bond fluctuation model[26] and the grand canonical simulation techniques[18] described briefly in Section 2 two of the fundamental difficulties can be overcome rather easily, the main topic here was to get around the remaining point (b). This was achieved by applying multiple-histogram extrapolation techniques recently formulated for spin systems[35] to polymer mixtures, thereby enhancing the amount of information extractable from a simulation run by at least one order of magnitude (see Section 3).

As also shown in Section 3, these techniques can easily be generalized to other parameters than temperature and chemical potential, and are therefore well suited to be applied to asymmetric mixtures. In fact, since with asymmetric monomer interaction potentials the critical point of unmixing moves away from the temperature axis ($\Delta\mu_c \neq 0$), the histogram extrapolations which allow continuous scans of two (or more) parameters over the entire critical region may be the only chance to find the critical point at all. Indeed, without histograms it would already be hard to find a sensible point in parameter space at which to run the simulation! But with the histogram method the procedure to locate the "optimal" simulation point is easy:

Use the histograms from the symmetric mixtures to extrapolate the order parameter susceptibility χ to a small asymmetry. Locate the maximum of χ as a function of the two parameters $(T, \Delta\mu)$. This maximum is already near the critical point of the asymmetric mixture and in any case is the best point to perform an additional simulation for the asymmetric mixture, since there the new histogram will be very broad. Now use the new histogram (combined with the old one) to extrapolate to even larger asymmetry and again locate the maximum of χ, etc. For a mixture of chains with length $N=32$ the maximum of χ for various asymmetry parameters λ (see Section 3.5) is off the temperature axis by an amount of $\Delta\mu = -0.23$ for $\lambda = 1.1$, already by $\Delta\mu = -1.3$ for $\lambda = 1.5$, and up to $\Delta\mu = -2.3$ for $\lambda = 2.0$,[36] showing drastically how hard it would be to find the critical point of asymmetric mixtures just by wildly guessing the simulation points without having continuous information over the critical region available!

Another advantage of the histograms is that one does not need to know what exactly are the best quantities to measure at the time the simulation runs. One just records histograms and, since the complete information about the phase transition is contained therein, later any desired function out of the many (sometimes new and unconventional) possibilities presented in Section 4 can be calculated within minutes on a work station.

As an example system for this study, I used symmetric polymer mixtures at density $(1-\phi_v)=0.5$ with chain lengths ranging from $N=16$

to $N=256$. The critical behavior of these systems is summarized in Table II. Here the exponents and critical amplitudes of the order parameter and the susceptibility for $N \geqslant 64$ are to be understood as *effective* quantities as mentioned in the text. The physical interpretation of these results can be found in refs. 44 and 36.

The histogram extrapolations together with suitable finite-size scaling functions from Section 4 provide powerful tools to extract reliable information about critical points, exponents, and amplitudes out of data with far less statistics than previously neccessary. Therefore even mixtures of relatively long chains can be investigated. Instead of enlarging N, another direction for which these new advantages may be exploited is to investigate mixtures with large asymmetries. There the computer time is mainly needed for canonical relaxations between two switches if the asymmetry is so large that the chain configurations of the A and B species are significantly different. Besides the already mentioned asymmetry in the monomer potentials, the rich possibilities of the bond fluctuation model can be used to simulate different chain stiffnesses, bond length distributions, or even different chain lengths.

APPENDIX. SPONTANEOUS SYMMETRIC BREAKING AND THE THERMODYNAMIC LIMIT

With finite-size scaling techniques as described in Section 4 the physics in the thermodynamic limit can be obtained from the finite systems with one important exception: There is no spontaneously broken symmetry of the order parameter distribution in the finite systems and it cannot be produced in the $L \to \infty$ limit of finite-size scaling. In the two-phase region below T_c the distribution of m is still fully symmetric with two peaks at $\pm m_0$ (see Fig. 5) if (as is the case here) the simulated systems are so small that the energy cost to build an percolating interface between a $+m_0$ and $-m_0$ domain, necessary to switch the average magnetization, is small enough to happen quite often during the simulation. Therefore all odd moments of the order parameter vanish, in striking contrast to the thermodynamic limit.

A common practice[39] to introduce spontaneous symmetry breaking "by hand" is to use the absolute value $|m|$ for odd moments, which should have the right limiting behavior

$$\langle |m^{2k-1}| \rangle_L \xrightarrow{L \to \infty} m_0^{2k-1}$$

To decide where to use m and where $|m|$ in the finite-size scaling techniques

of Section 4, let us assume that $P(m)$ in the thermodynamic limit is a Gaussian peaked around m_0,

$$P(m) = \frac{1}{(2\pi\sigma^2)^{1/2}} \exp\left[-\frac{1}{2\sigma^2}(m-m_0)^2 \right] \tag{A1}$$

with

$$m_0 = \langle m \rangle, \qquad \sigma^2 = \langle m^2 \rangle - \langle m \rangle^2 = k_B T \chi L^{-d} \tag{A2}$$

This is also the limiting distribution for the finite systems of computer simulations *in the one-phase region*, i.e., for symmetric mixtures in the region where $T > T_c$ or $\Delta\mu \neq 0$. But in the two-phase region $T < T_c$, $\Delta\mu = 0$ the $L \to \infty$ limit from finite systems is not the above asymmetric distribution, but (to a very good approximation, except close to $m = 0$[58,39])

$$P(m) = \frac{1}{(2\pi\sigma^2)^{1/2}} \left\{ \frac{1}{2} \exp\left[-\frac{1}{2\sigma^2}(m-m_0)^2 \right] + \frac{1}{2} \exp\left[-\frac{1}{2\sigma^2}(m+m_0)^2 \right] \right\} \tag{A3}$$

With these two distributions any function of order parameter moments can be calculated in the thermodynamic limit or in the limit $L \to \infty$ from finite

Table III. The Limits $L \to \infty$

	$L \to \infty$ *without* symmetry breaking			$L \to \infty$ *with* symmetry breaking
	Two phases:	One phase		Two phases:
	$\Delta\mu = 0,\ T < T_c$	$\Delta\mu = 0,\ T > T_c$	$\Delta\mu \neq 0$	$\Delta\mu = 0,\ T < T_c$
$\langle m \rangle$	0	0	m_0	$m_0 = \pm\lvert m_0 \rvert$
$\langle \lvert m \rvert \rangle$	$\lvert m_0 \rvert$	$(2/\pi)^{1/2}\sigma$	$\lvert m_0 \rvert$	$\lvert m_0 \rvert$
$\langle m^2 \rangle$	$\sigma^2 + m_0^2$	σ^2	$\sigma^2 + m_0^2$	$\sigma^2 + m_0^2$
$L^d(\langle m^2 \rangle - \langle m \rangle^2)$	∞?	$k_B T\chi$	$k_B T\chi$	$k_B T\chi$
$L^d(\langle m^2 \rangle - \langle \lvert m \rvert \rangle^2)$	$k_B T\chi$	$(1-2/\pi)\, k_B T\chi$	$k_B T\chi$	$k_B T\chi$
$\langle m^2 \rangle / \langle m \rangle^2$	$(m_0^2 + \sigma^2)/0$?	$\sigma^2/0 \to 0/0$?	1	1
$\langle m^2 \rangle / \langle \lvert m \rvert \rangle^2$	1	$\pi/2$	1	1
$\langle m^4 \rangle / \langle m^2 \rangle^2$	1	3	1	1
$W_1(L_2, L_1, m)$	$\sim\ln(0/0)$?	$\sim\ln(0/0)$?	0	0
$W_1(L_2, L_1, \lvert m \rvert)$	0	$d/2$	0	0

systems and by comparison one can decide where to use m and where $|m|$. The results for some of the functions in Section 4 are presented in Table III. The underscored quantities in Table III are the ones actually used in the analysis. Note that the rule of thumb "uses $|m|$ for all odd moments" may lead to wrong critical amplitudes for fluctuations like the susceptibility above T_c. The factor $1-2/\pi$ between the right and wrong way of measuring the susceptibility above T_c is indeed confirmed by the simulations (see Figs. 7 and 10). Of course, if one is interested only in critical exponents and not in the amplitudes, such factors do not matter.

ACKNOWLEDGMENTS

This research was supported in part by the Deutsche Forschungsgemeinschaft under grant No. Bi314/3-1. The author is particularly grateful to K. Binder, D. P. Landau, and A. Ferrenberg for many fruitful and stimulating discussions. Thanks are also due to the Höchstleistungsrechenzentrum (HLRZ) Jülich and to the Regionales Hochschulrechenzentrum Kaiserslautern (RHRK) for grants of computer time on the CRAY-YMP and Fujitsu-VP100 vector processors.

REFERENCES

1. P. J. Flory, *Principles of Polymer Chemistry* (Cornell University Press, Ithaca, New York, 1986).
2. D. J. Walsh, J. S. Higgins, and S. Rostami, *Macromolecules* **16**:388 (1983).
3. H. Ito, T. P. Russel, and G. Wignall, *Macromolecules* **20**:2213 (1987).
4. F. S. Bates, *Macromolecules* **20**:2221 (1987).
5. R. L. Scott, *J. Chem. Phys.* **17**:279 (1949).
6. P. G. de Gennes, *J. Phys. Lett.* (Paris) **38**:L441 (1977).
7. A. Budkowski, U. Steiner, J. Klein, and G. Schatz, *Phys. Rev. Lett.* (1991).
8. P. J. Flory, *J. Chem. Phys.* **9**:660 (1941).
9. M. L. Huggins, *J. Chem. Phys.* **9**:440 (1941).
10. E. A. Guggenheim, *Proc. R. Soc. A* **183**:203, 231 (1944).
11. W. G. Madden, A. I. Pesci, and K. F. Freed, *Macromolecules* **23**:1181 (1990).
12. J. E. G. Lipson, *Macromolecules* **24**:1334 (1991).
13. V. L. Ginzburg, *Sov. Phys. Solid State* **2**:1824 (1960).
14. J. F. Joanny, *J. Phys. A* (Paris) **11**:L117 (1978).
15. K. Binder, *Colloid Polym. Sci.* **265**:27 (1987).
16. P. G. de Gennes, *Scaling Concepts in Polymer Physics* (Cornell University Press, Ithaca, New York, 1979).
17. F. S. Bates, J. H. Rosedale, P. Stepanek, T. P. Lodge, P. Wiltzius, G. H. Fredrickson, and R. P. Hjelm, Jr., *Phys. Rev. Lett.* **65**:1893 (1990).
18. A. Sariban and K. Binder, *J. Chem. Phys.* **86**:5859 (1987); *Macromolecules* **21**:711 (1988).
19. A. Sariban and K. Binder, *Colloid Polym. Sci.* **267**:469 (1989).
20. K. Kremer and K. Binder, *Computer Phys. Rep.* **8**:211 (1988).

21. K. Binder, *Monte Carlo Simulations of Polymer Systems* (Springer-Verlag, Heidelberg, 1988), p. 84.
22. K. Binder, ed., *Monte Carlo Methods in Statistical Physics* (Springer-Verlag, Heidelberg, 1986).
23. K. Binder, ed., *Applications of the Monte Carlo Method in Statistical Physics* (Springer-Verlag, Heidelberg, 1987).
24. K. Binder, *J. Chem. Phys.* **79**:6387 (1983).
25. W. Paul, K. Binder, D. W. Heermann, and K. Kremer, *J. Phys.* (Paris) **II-1**:37 (1991).
26. H.-P. Deutsch and K. Binder, *J. Chem. Phys.* **94**:2294 (1991).
27. K. Binder, H.-P. Deutsch, and A. Sariban, *J. Non-Cryst. Solids* **131–133**:635 (1991).
28. P. H. Verdier and W. H. Stockmayer, *J. Chem. Phys.* **36**:227 (1962).
29. F. T. Wall and F. Mandel, *J. Chem. Phys.* **63**:4592 (1975).
30. F. S. Bates, G. D. Wignall, and W. C. Koehler, *Phys. Rev. Lett.* **55**:2425 (1985); *Macromolecules* **19**:934 (1986).
31. I. Carmesin and K. Kremer, *Macromolecules* **21**:2819 (1988).
32. H.-P. Deutsch and R. Dickman, *J. Chem. Phys.* **93**:8983 (1990).
33. Z. W. Salsburg, J. D. Jacobsen, W. Fickett, and W. W. Wood, *J. Chem. Phys.* **30**:64 (1959); D. A. Chesnut and Z. W. Salsburg, *J. Chem. Phys.* **38**:2861 (1963).
34. G. Bhanot, S. Black, P. Carter, and R. Salvador, *Phys. Lett. B* **183**:331 (1987); G. Bhanot, K. M. Bitar, S. Black, P. Carter, and R. Salvador, *Phys. Lett. B* **187**:381 (1987); G. Bhanot, K. M. Bitar, P. Carter, and R. Salvador, *Phys. Lett. B* **188**:246 (1987).
35. A. M. Ferrenberg and R. H. Swendsen, *Phys. Rev. Lett.* **61**:2635 (1988); **63**:1195 (1989).
36. H.-P. Deutsch, Dissertation, Johannes Gutenberg Universität Mainz, unpublished (1991); *Polymer*, in press (1992); *Macromolecular Chem.*, in press (1992).
37. K. Huang, *Statistical Mechanics* (Wiley, New York, 1987).
38. N. Metropolis, A. W. Rosenbluth, M. N. Rosenbluth, A. H. Teller, and E. Teller, *J. Chem. Phys.* **21**:1087 (1953).
39. K. Binder and D. W. Heermann, *Monte Carlo Simulations in Statistical Physics* (Springer-Verlag, Heidelberg, 1988).
40. J. M. Rickman and S. R. Phillpot, *Phys. Rev. Lett.* **66**:349 (1991).
41. N. Madras and A. Sokal, *J. Stat. Phys.* **50**:109 (1988).
42. H. Flyvbjerg and H. G. Petersen, *J. Chem. Phys.* **91**:461 (1989).
43. C. H. Bennett, *J. Comput. Phys.* **22**:245 (1976).
44. H.-P. Deutsch and K. Binder, Critical properties of polymer mixtures, *Macromolecules* (1992).
45. H. E. Stanley, *Introduction to Phase Transitions and Critical Phenomena* (Oxford Science Publishers, Oxford, 1971).
46. S. K. Ma, *Modern Theory of Critical Phenomena* (Benjamin/Cummings, Reading, Massachusetts, 1976).
47. K. Binder, in *Materials Science and Technology*, R. W. Cahn, P. Haasen, and E. J. Kramer, eds. (VCH, Weinheim, Germany, 1991).
48. B. Widom, *J. Chem. Phys.* **43**:3898 (1965).
49. D. Stauffer, M. Ferer, and M. Wortis, *Phys. Rev. Lett.* **29**:345 (1972).
50. G. S. Pawley, R. H. Swendsen, D. J. Wallace, and K. G. Wilson, *Phys. Rev. B* **29**:4030 (1984).
51. K. Binder, M. Nauenberg, V. Privman, and A. P. Young, *Phys. Rev. B* **31**:1498 (1985).
52. V. Privman and M. E. Fisher, *J. Stat. Phys.* **33**:385 (1983).
53. K. Binder, *Z. Phys. B* **61**:13 (1985).
54. M. E. Fisher, in *Critical Phenomena, Proceedings 1970 E. Fermi International School of Physics*, Vol. 51, M. S. Green, ed. (Academic Press, New York, 1971).

55. M. N. Barber, in *Phase Transitions and Critical Phenomena*, Vol. 8, C. Domb and M. S. Green, eds. (Academic Press, New York, 1983).
56. J. L. Cardy, ed., *Finity Size Scaling* (North-Holland, Amsterdam, 1988).
57. V. Privman, in *Finite Size Scaling and Numerical Simulation of Statistical Systems*, V. Privman, ed. (World Scientific, Singapore, 1990).
58. K. Binder, *Z. Phys. B* **43**:119 (1981); *Phys. Rev. Lett.* **47**:693 (1981).
59. A. M. Ferrenberg and D. P. Landau, Critical behavior of the three dimensional Ising model: A high resolution study, Preprint.